



Elementos finitos sin miedo: *Una herramienta para entender el café*

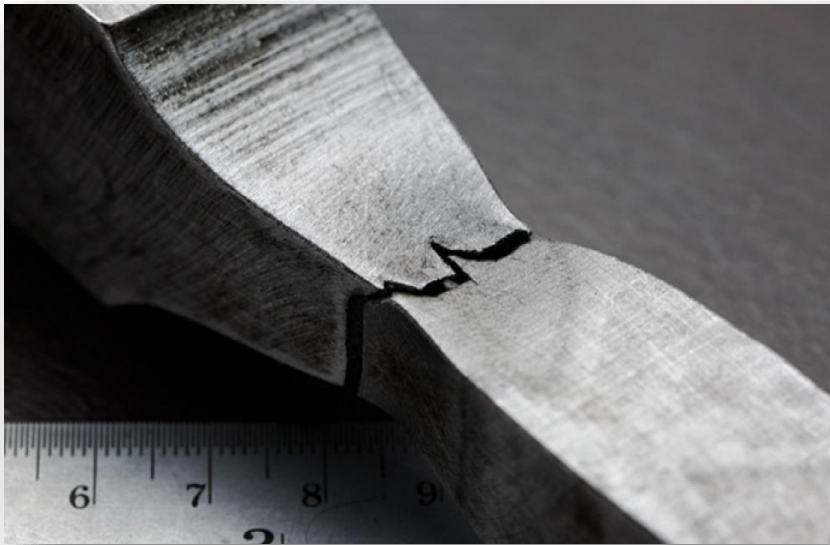
Eduardo Duque Dussán, Ph.D.
Disciplina de Ingeniería

SABEMOS
LO QUE HACEMOS





¿Cómo sabemos que algo va a fallar?



Mismo problema, diferente escala



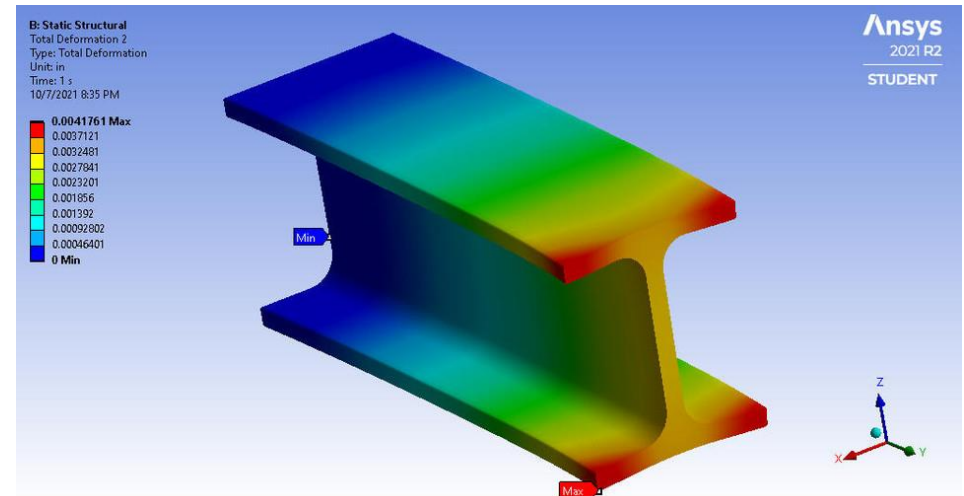
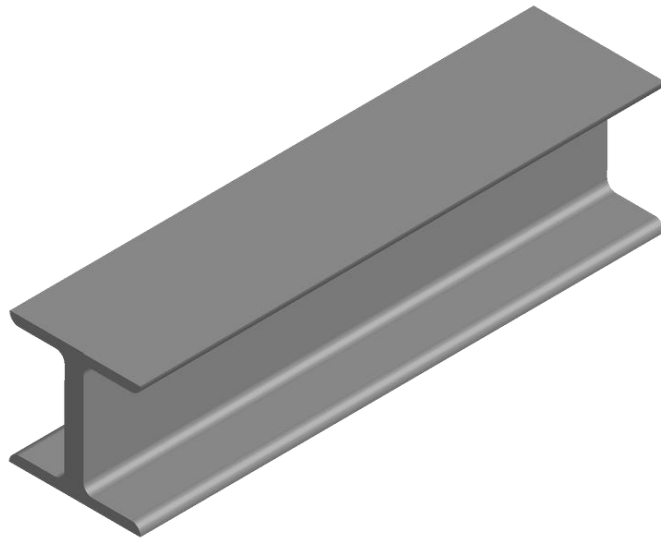
Lo importante no siempre se ve

Lo que vemos

- Forma
- Movimiento
- Superficie

Lo que no vemos

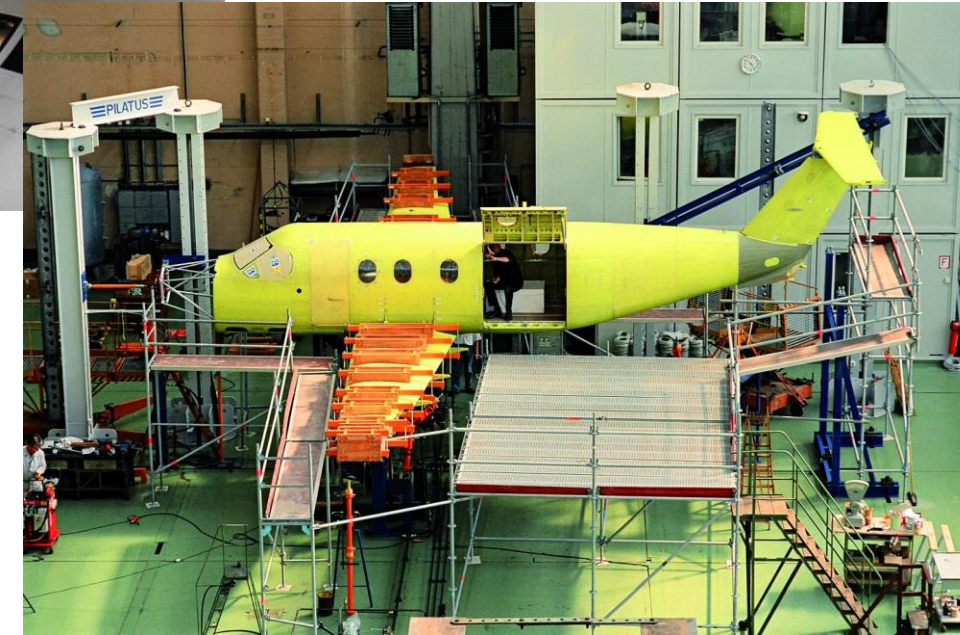
- Esfuerzos
- Deformaciones internas
- Gradientes





Antes... había que construir para entender

- Construir
- Medir
- Ajustar
- Repetir



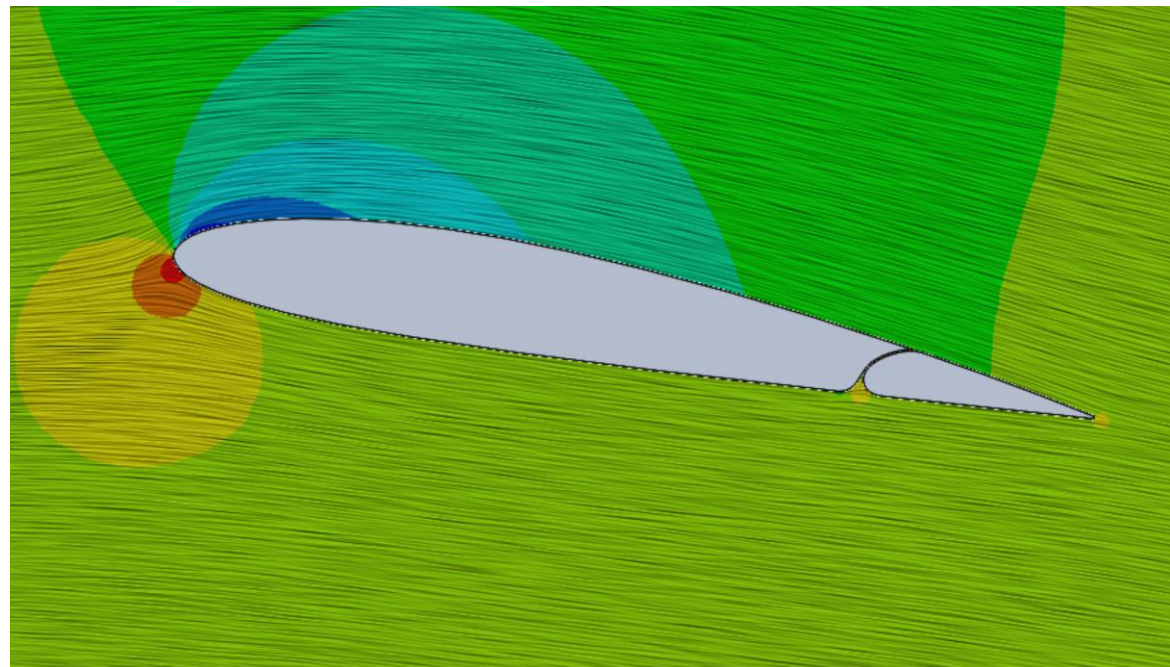
Prueba y error



Hoy... podemos entender antes de construir



- Simular
- Analizar
- Optimizar
- **Construir**

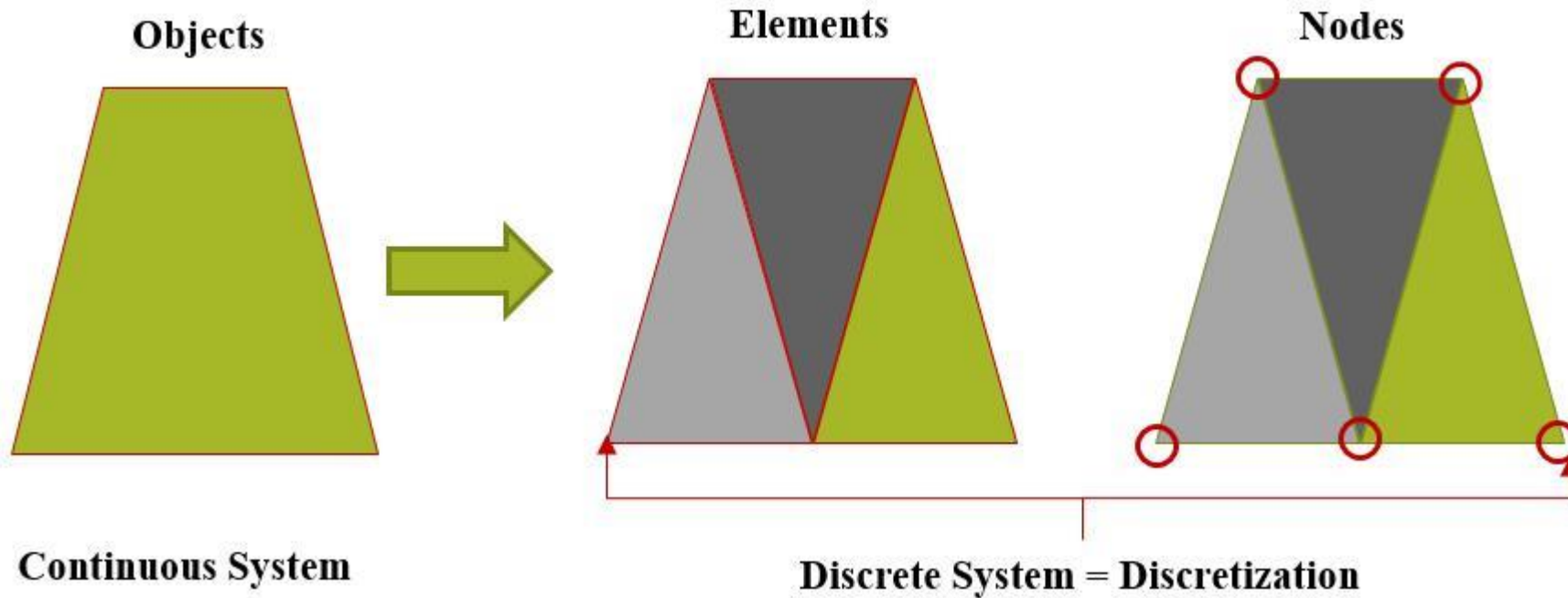


Diseñar sin construir



Método de los elementos finitos (FEM)

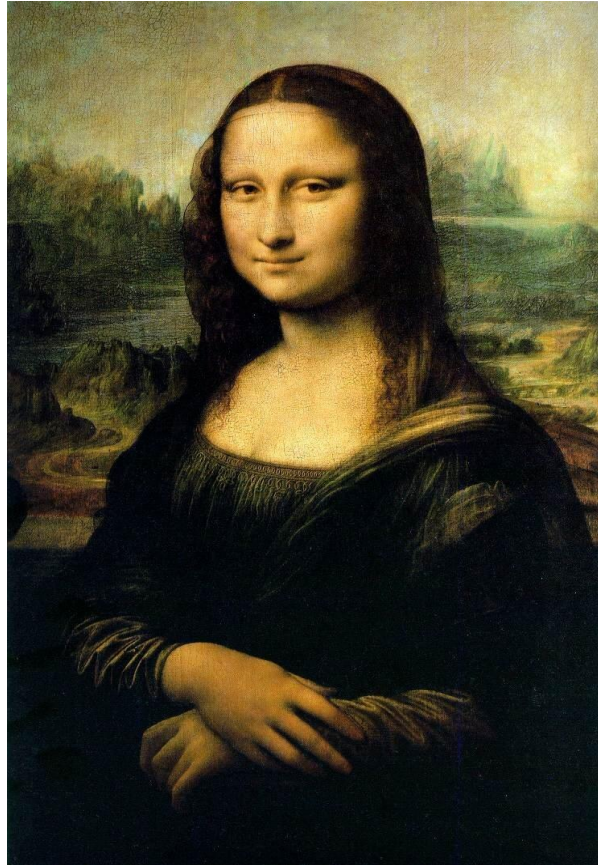
Una herramienta para entender lo que no vemos





Entender dividiendo

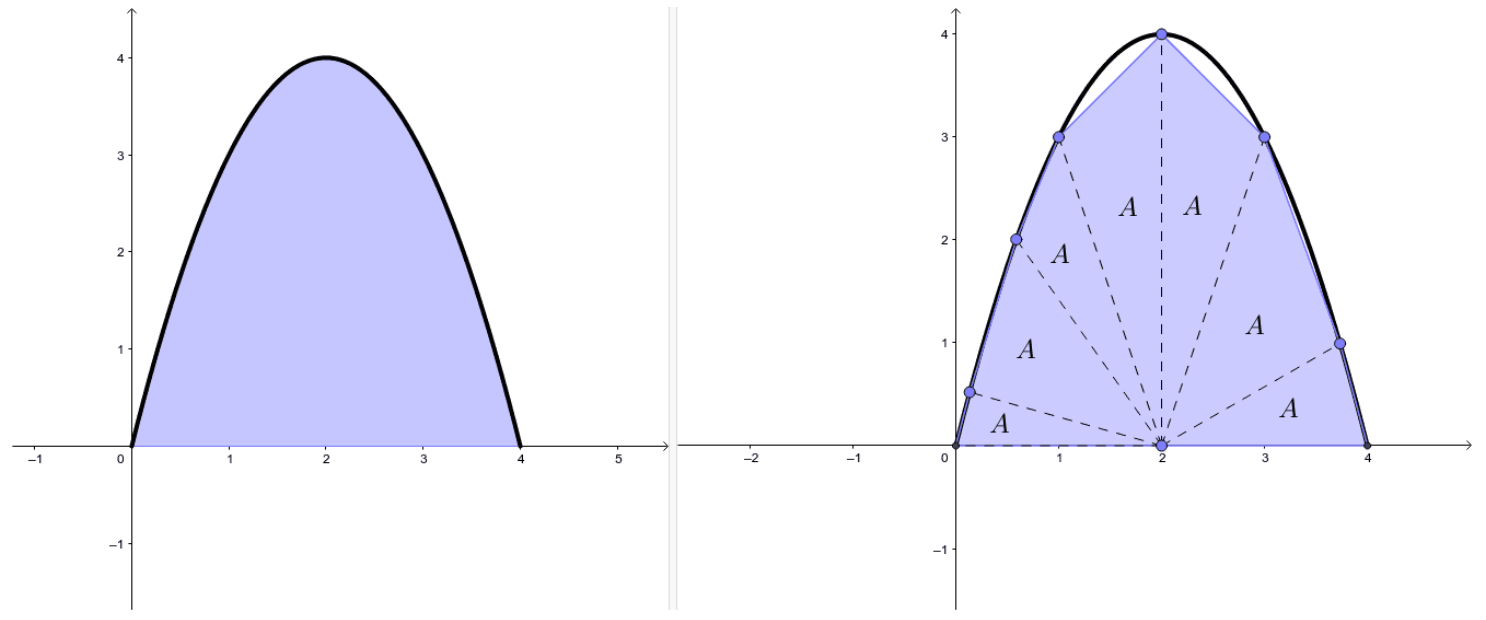
Un problema complejo = muchos problemas simples





Historia

Esto no es del todo nuevo



“Toda magnitud finita puede ser agotada mediante la sustracción de una cantidad determinada”

Eudoxo de Cnido
c. 390 a. C.-c. 337 a. C.





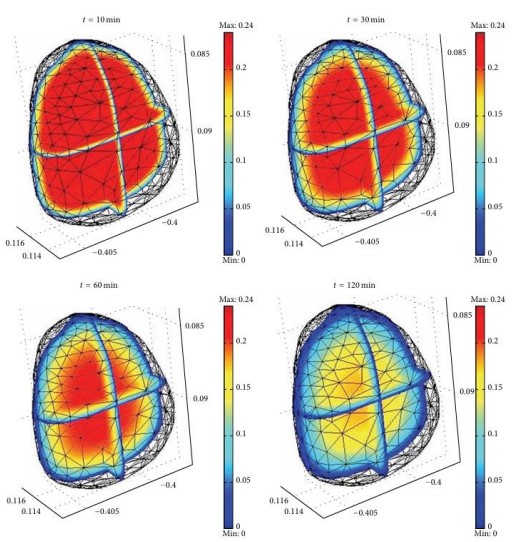
Historia: Transición matemática

De la geometría a los fenómenos físicos

- Eudoxo de Cnido (~400 a.C.) → Aproximación geométrica
- Siglos XVII–XIX → Nacen las ecuaciones diferenciales ¿para qué?

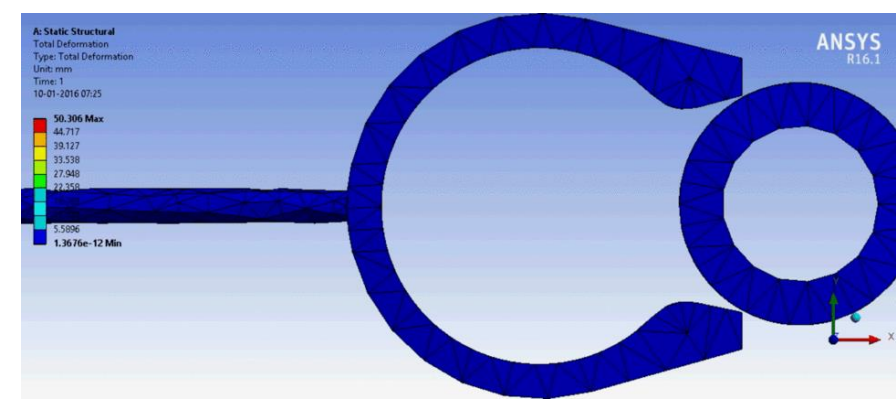
Temperatura

$$\frac{\partial T}{\partial t} = \alpha \nabla^2 T$$



Deformación

$$\nabla \cdot \sigma + f = 0$$

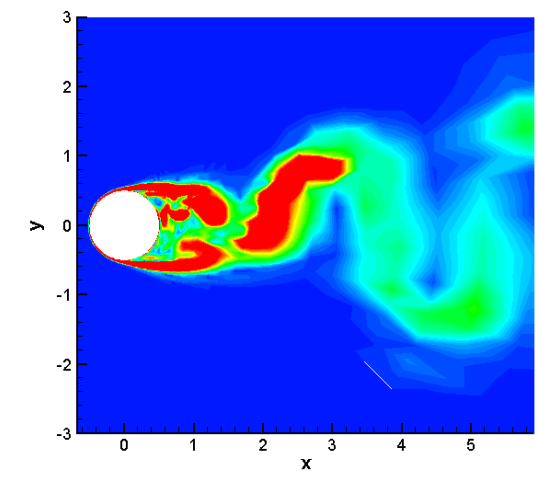


Los problemas crecieron... y las soluciones exactas dejaron de existir

<http://dx.doi.org/10.1155/2013/579452>

Flujo

$$\rho(\mathbf{u} \cdot \nabla)\mathbf{u} = -\nabla p + \mu \nabla^2 \mathbf{u}$$





El límite de las ecuaciones diferenciales



Cuando las ecuaciones no se pueden resolver

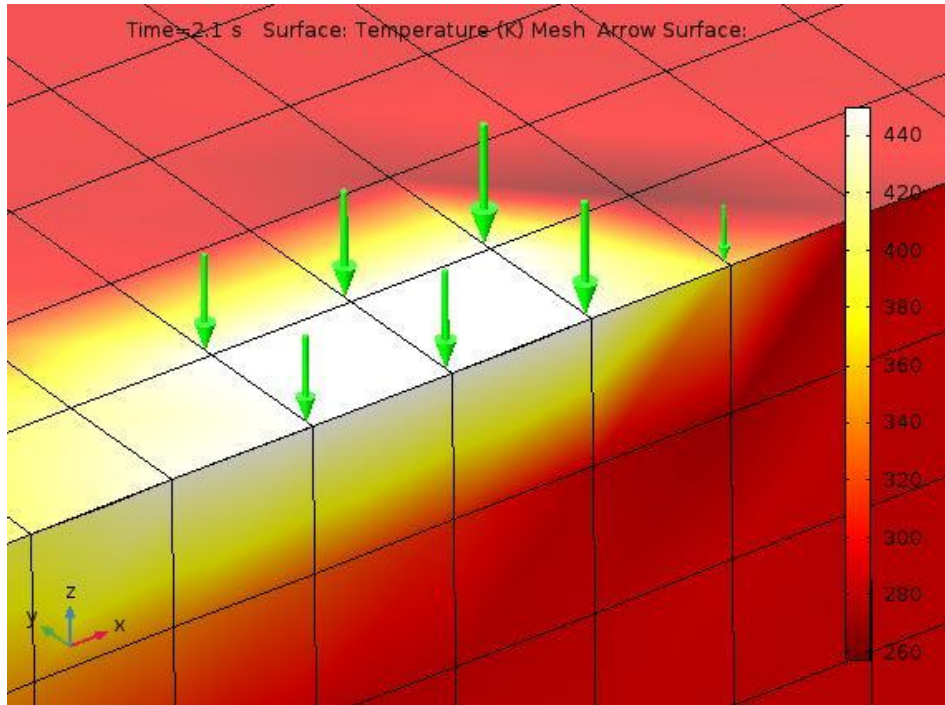
Temperatura

$$\frac{\partial T}{\partial t} = \alpha \nabla^2 T$$

Dependencia:

- Espacio
- Tiempo
- Condiciones reales

Solución exacta solo en casos ideales



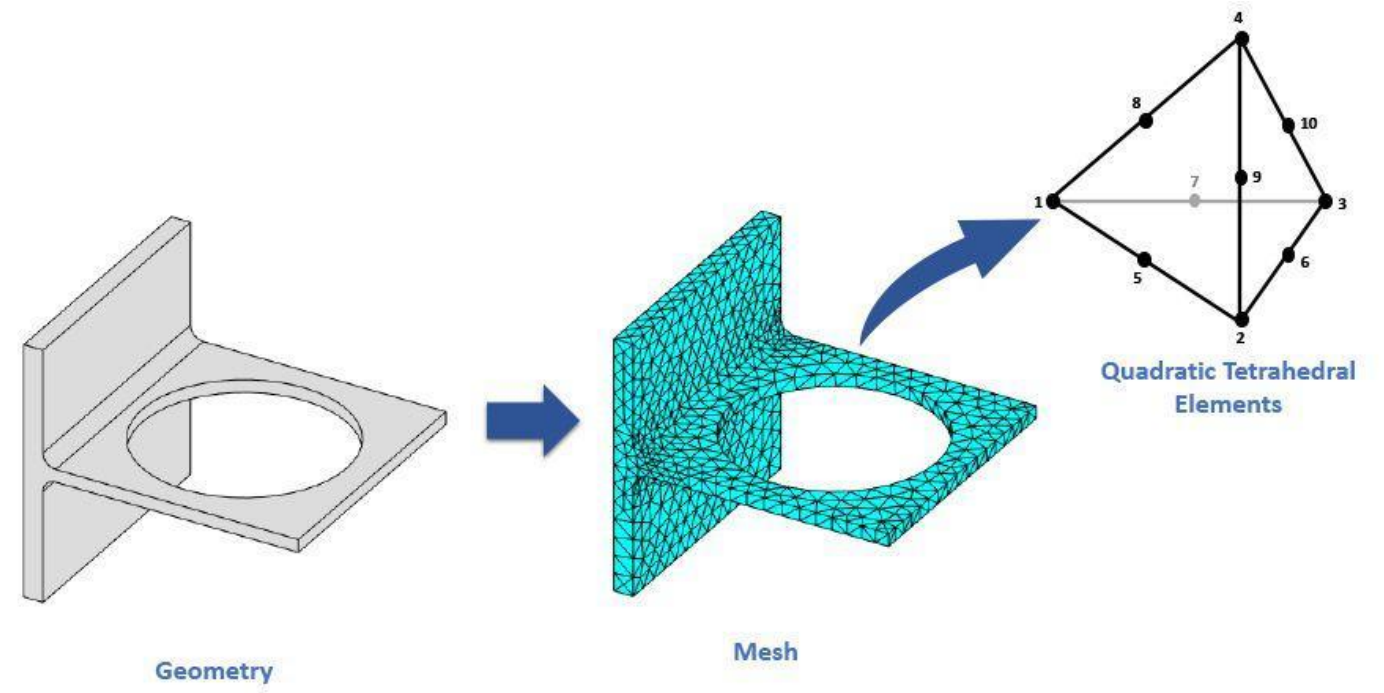


Entonces aproximamos

Convertimos lo continuo en discreto

- Dividir el dominio
- Evaluar localmente
- Resolver numéricamente

Resolver exactamente no es posible... aproximar sí



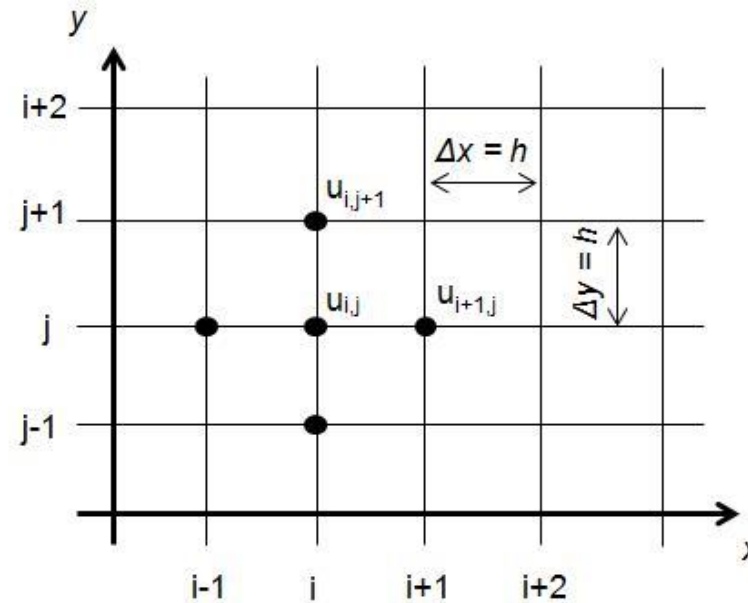


Diferencias finitas

Aproximar derivadas usando diferencias

- Se usan puntos en una malla regular
- Se evalúan valores en nodos
- Se reemplazan derivadas por diferencias

La derivada se convierte en una diferencia



$$\frac{dT}{dx} \approx \frac{T_{i+1} - T_i}{\Delta x}$$



El problema de las diferencias finitas

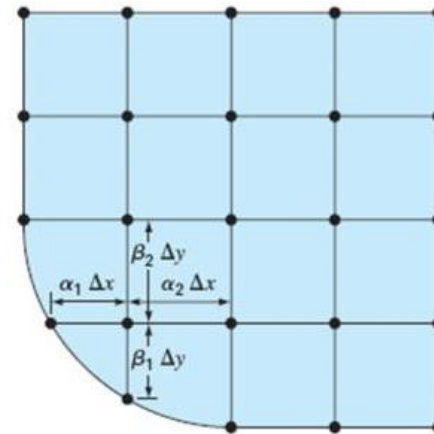


¿Qué pasa si la geometría no es simple?

- Requiere mallas regulares
- Difícil en geometrías complejas
- Problemas con bordes irregulares

La realidad no es una malla perfecta

Fronteras Irregulares



1er Derivada :

$$\left(\frac{\partial T}{\partial x}\right)_{i-1,j} \cong \frac{T_{i,j} - T_{i-1,j}}{\alpha_1 \Delta x}$$

$$\left(\frac{\partial T}{\partial x}\right)_{i,j+1} \cong \frac{T_{i+1,j} - T_{i,j}}{\alpha_2 \Delta x}$$

2da: Derivada :

$$\frac{\partial^2 T}{\partial x^2} = \frac{\partial}{\partial x} \left(\frac{\partial T}{\partial x} \right) = \frac{\left(\frac{\partial T}{\partial x}\right)_{i,j+1} - \left(\frac{\partial T}{\partial x}\right)_{i-1,j}}{\frac{\alpha_1 \Delta x + \alpha_2 \Delta x}{2}} \Rightarrow \frac{\partial^2 T}{\partial x^2} = 2 \frac{\frac{T_{i-1,j} - T_{i,j}}{\alpha_1 \Delta x} - \frac{T_{i+1,j} - T_{i,j}}{\alpha_2 \Delta x}}{\alpha_1 \Delta x + \alpha_2 \Delta x}$$



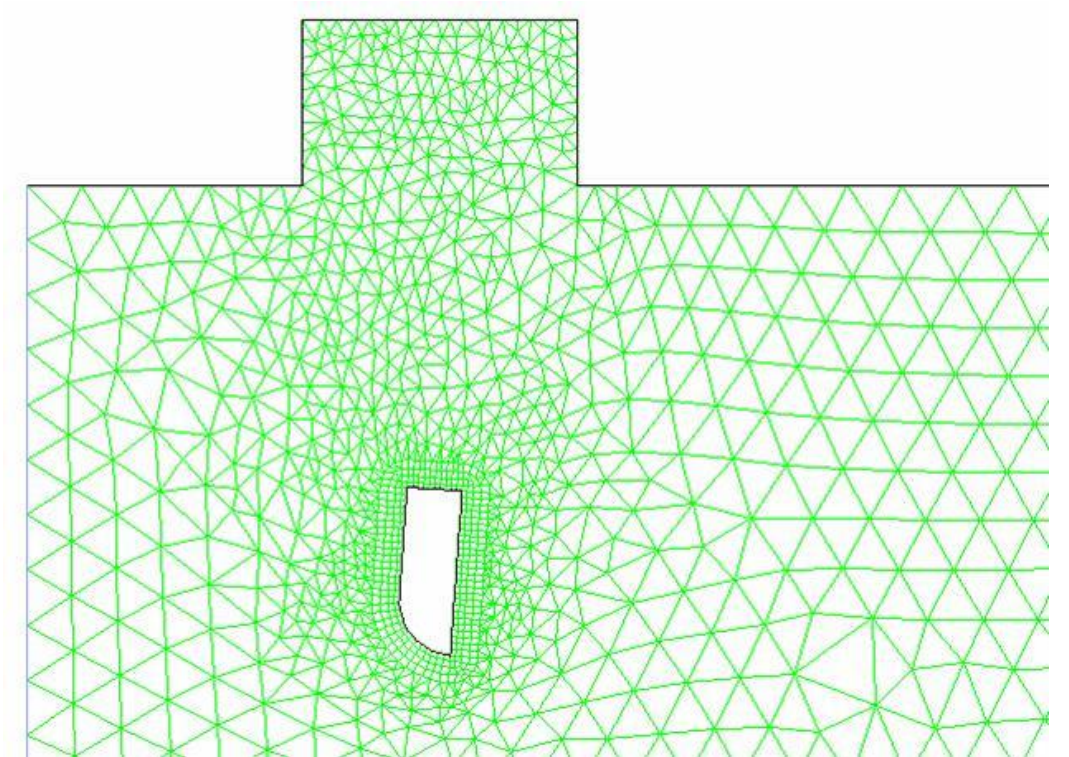
Entonces... aparecen los elementos finitos

La malla se adapta a la geometría



- Dividimos la geometría en elementos
- Nos adaptamos a cualquier forma
- Resolución local → solución global

Ya no forzamos la realidad... nos adaptamos a ella





¿Cómo funciona el método de elementos finitos?



Resolver localmente para entender globalmente

Discretización

Dividir el dominio en elementos

Nodos

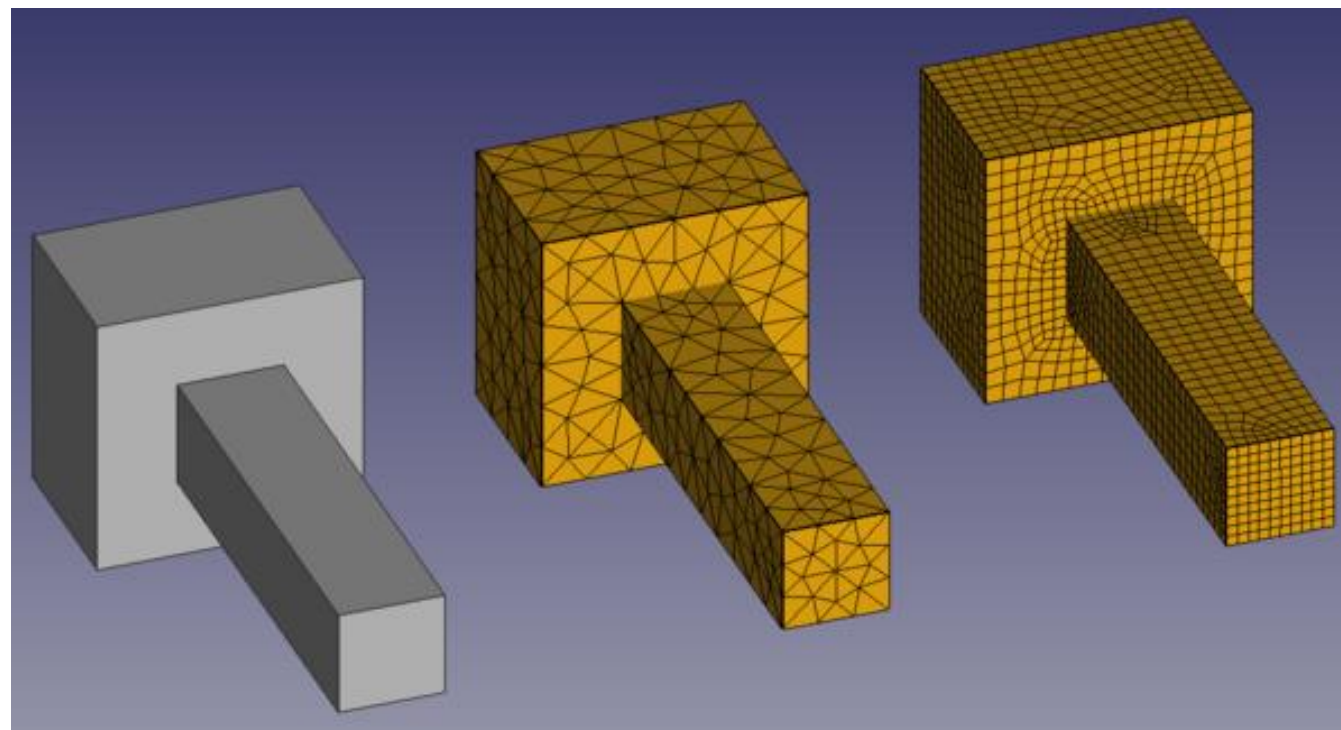
Puntos donde se calculan las variables

Ecuaciones locales

Cada elemento tiene su propio comportamiento

Ensamblaje

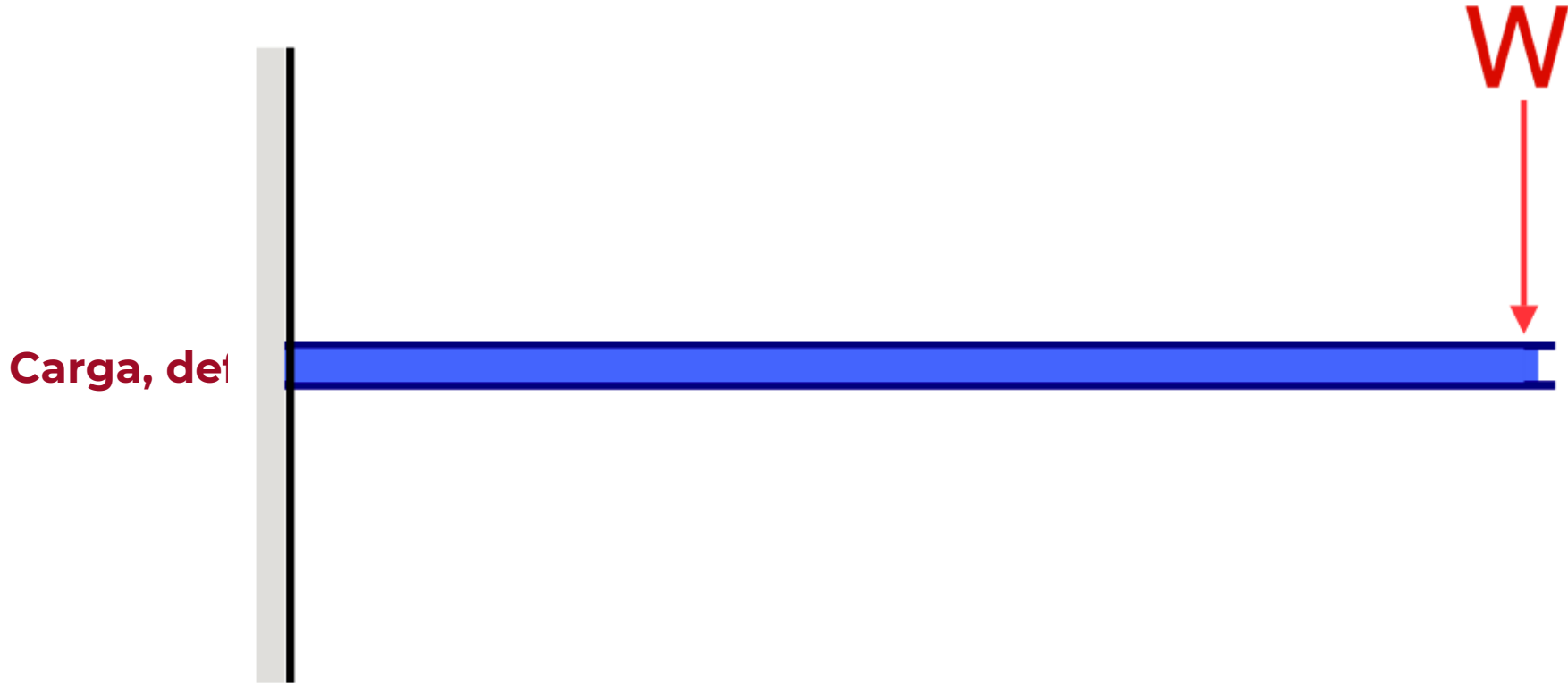
Se conectan todos los elementos → sistema global





Ejemplo: una viga en voladizo

¿Dónde se concentra el esfuerzo?



RESULTADOS

ANÁLISIS

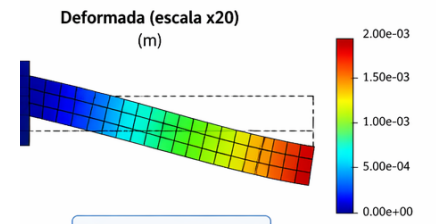
$$M_{max} = PL = 1000 \text{ N}\cdot\text{m}$$

$$\sigma_{max} = \frac{M_{max} c}{I} = \frac{1000(0.05)}{8.33 \times 10^{-6}}$$

$$\sigma_{max} = 6.00 \times 10^6 \text{ Pa} = 6.00 \text{ MPa}$$

$$\delta_{max} = \frac{PL^3}{3EI} = \frac{1000(1)^3}{3(210 \times 10^9)(8.33 \times 10^{-6})}$$

$$\delta_{max} = 1.98 \text{ mm}$$



$\delta_{max, FEM} = 1.97 \text{ mm}$
(en el extremo libre)

✓ Los resultados del modelo FEM coinciden muy bien con la solución analítica.

Deflexión máxima (mm)	1.98	1.97	0.51 %
-----------------------	------	------	--------



¿Qué nos dice el resultado?

- El esfuerzo máximo está en el empotramiento
- La deformación aumenta hacia el extremo libre
- **La falla ocurre donde el material no resiste**

VIGA EN VOLADIZO – PERFIL EN I | ANÁLISIS FEM

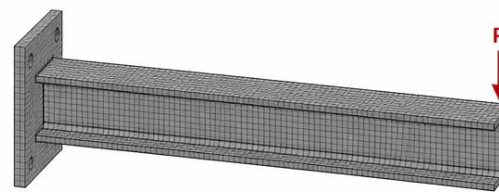
1. MODELO

Viga en voladizo – Perfil en I
Carga puntual en el extremo libre



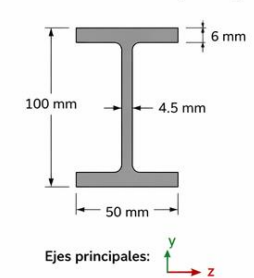
Propiedades	
E	210 GPa
ν	0.30
L	1.0 m
P	1000 N
Perfil en I (IPN 100)	
A	1260 mm ²
I_y	$2.02 \times 10^{-6} \text{ m}^4$
I_z	$1.23 \times 10^{-7} \text{ m}^4$

2. MALLA FEM

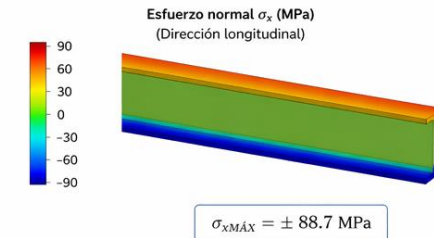
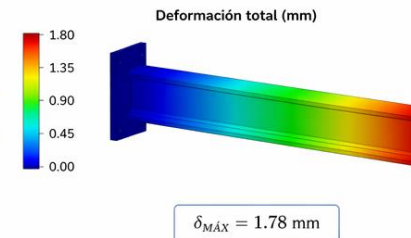
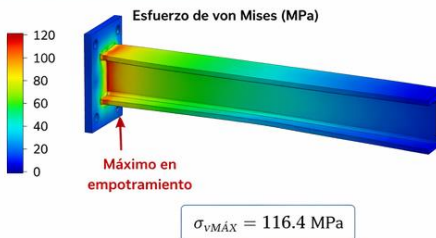


Tipo de elemento: Sólido 3D (Hexaédrico)
Nodos: 28,512
Elementos: 18,360

Sección transversal (IPN 100)

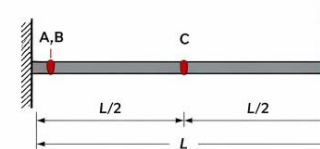


3. RESULTADOS FEM



4. VALORES EN PUNTOS CLAVE

Punto	Ubicación	σ_x (MPa)	δ (mm)
A	Empotramiento (fibra superior)	116.4	0.00
B	Empotramiento (fibra inferior)	116.1	0.00
C	Mitad de la viga (fibra superior)	38.2	0.44
D	Extremo libre (fibra superior)	0.8	1.78



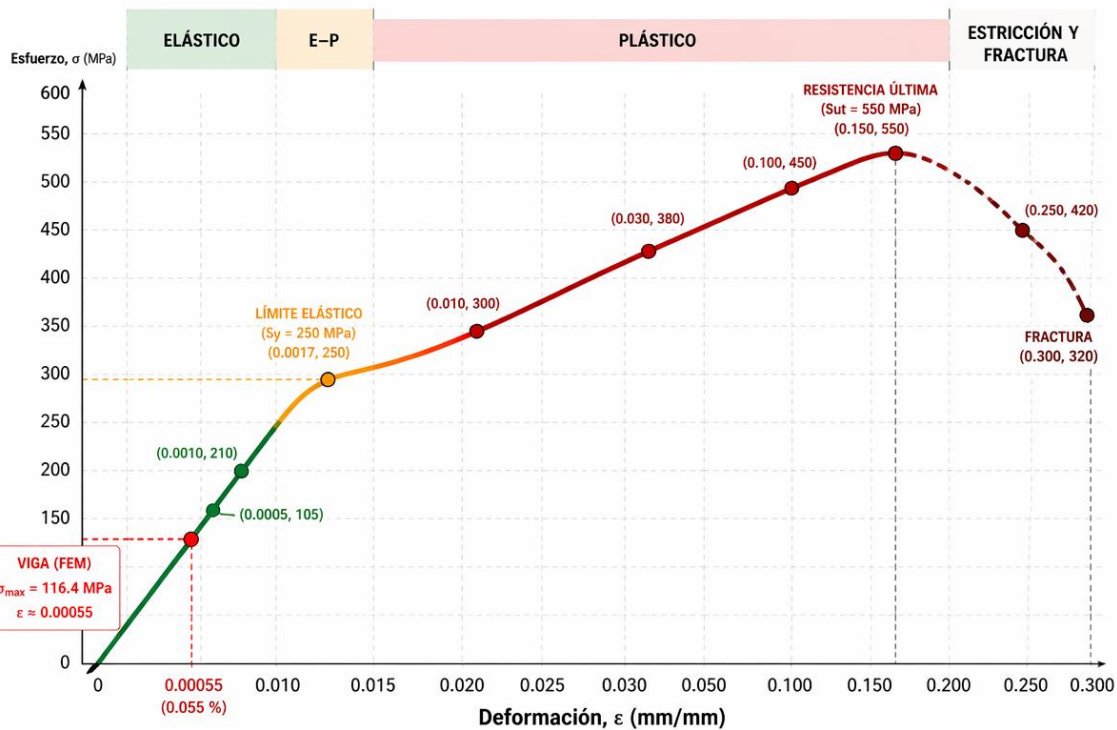
5. RESUMEN

- El máximo esfuerzo se presenta en el empotramiento.
- La deformación aumenta linealmente hacia el extremo libre.
- La distribución de esfuerzos normal σ_x muestra tracción en la fibra superior y compresión en la inferior.

✓ El modelo FEM captura correctamente el comportamiento esperado de una viga en voladizo de perfil en I.

La falla ocurre donde el material no resiste

CURVA ESFUERZO – DEFORMACIÓN DEL ACERO ESTRUCTURAL



Deformación, ϵ (mm/mm)	0	0.0005	0.0010	0.0017	0.005	0.010	0.030	0.050	0.100	0.150	0.250	0.300
Esfuerzo, σ (MPa)	0	105	210	250	280	300	380	420	450	550	420	320

— Región elástica (se recupera) — Zona elasto-plástica (inicio de fluencia) — Región plástica (deformación permanente) — Estricción y fractura

PROPIEDADES DEL ACERO

- Módulo de elasticidad, $E = 210 \text{ GPa}$
- Límite elástico, $S_y = 250 \text{ MPa}$
- Resistencia última, $S_{ut} = 550 \text{ MPa}$

RESULTADO DE LA VIGA (FEM)

$\sigma_{\max} = 116.4 \text{ MPa}$
 $\epsilon \approx 0.00055$ (0.055 %)
 Este punto está en la región **ELÁSTICA**

COMPARACIÓN

$\sigma_{\max} = 116.4 \text{ MPa}$
 $S_y = 250 \text{ MPa}$
 $\sigma_{\max} < S_y \rightarrow 116.4 < 250$
 La viga trabaja en la **REGIÓN ELÁSTICA**
 No se espera deformación plástica permanente.

INTERPRETACIÓN

El esfuerzo máximo obtenido con FEM (116.4 MPa) es menor que el límite elástico del acero (250 MPa).

La viga se deformará elásticamente y al retirar la carga recuperará su forma.

- El material tiene un límite
- No puede soportar cualquier esfuerzo
- Si el esfuerzo supera ese límite → falla

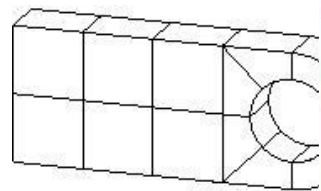
Límite elástico (S_y)
 Resistencia última (S_{ut})



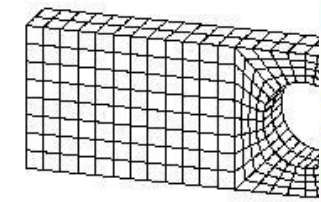
La malla: donde todo empieza

Una mala malla = malos resultados (aunque el modelo sea correcto)

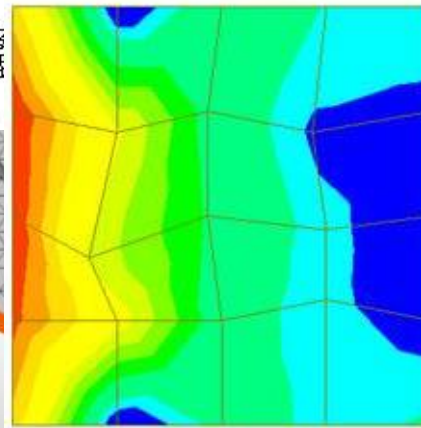
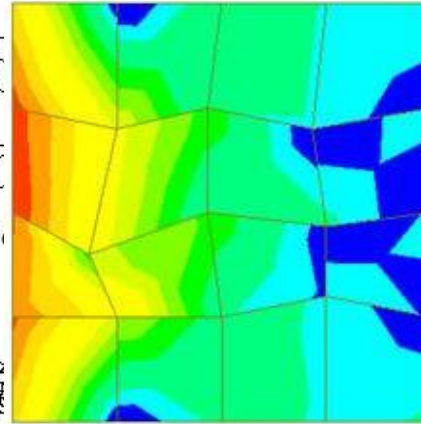
- La malla define cómo “vemos” el problema
- Divide la geometría en elementos
- Cada elemento resuelve una parte



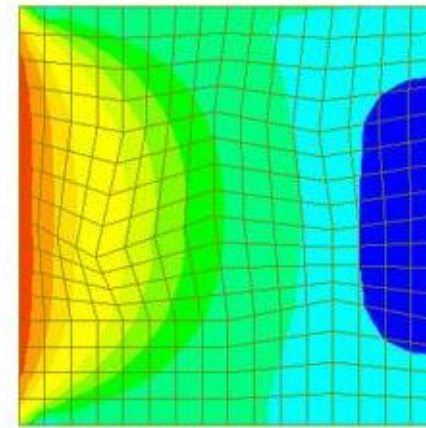
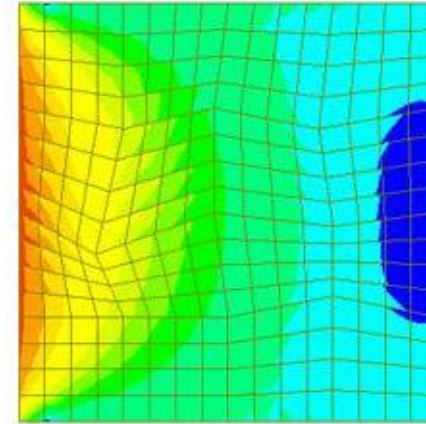
Coarse mesh (14 elements)



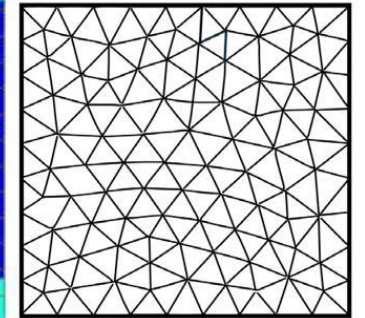
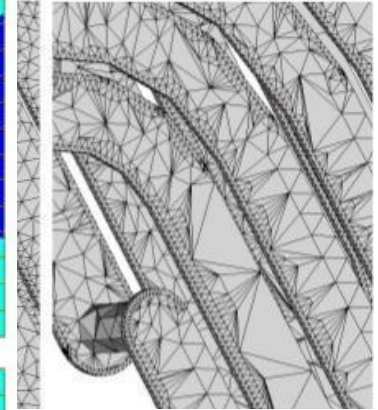
Fine mesh (448 elements)



(a) Unrefined mesh



(b) Refined mesh



Unstructured mesh



¿Cómo mejoramos la solución en FEM?



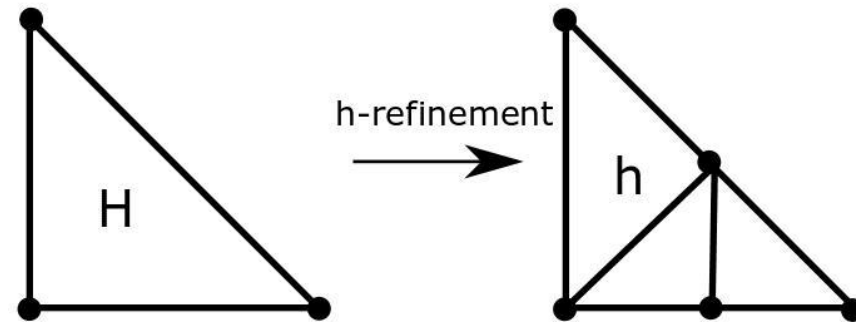
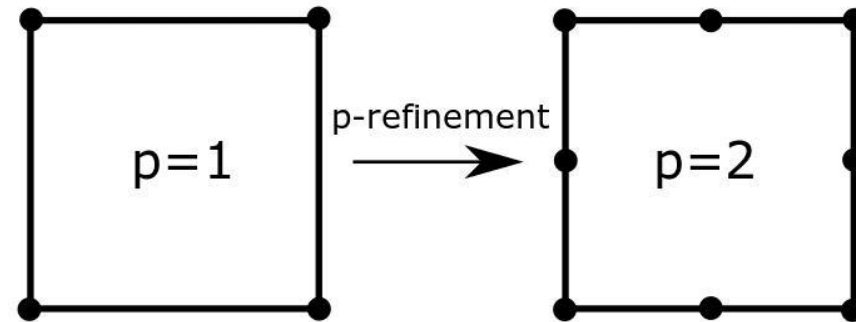
Dos caminos

- **p-refinement (refinamiento en orden)**

- Aumentar el orden del polinomio dentro del elemento
- Mismo elemento
- Más precisión dentro del elemento

- **h-refinement (refinamiento en tamaño)**

- Reducir el tamaño de los elementos
- Más elementos
- Más resolución



- $h \rightarrow$ más píxeles
- $p \rightarrow$ mejor calidad por píxel



Calidad de la malla: no todo mesh es bueno



Una buena malla respeta direcciones, forma y proporciones

Ortogonalidad

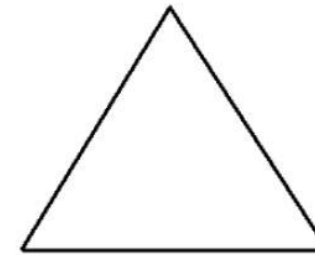
- Elementos alineados con la geometría y el flujo
- Baja ortogonalidad → direcciones mal representadas

Skewness (distorsión)

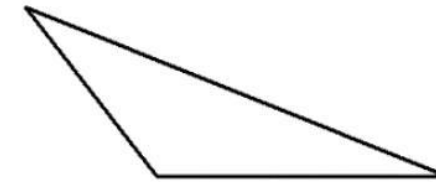
- Qué tan “torcido” está el elemento
- Alto skewness → errores numéricos

Aspect ratio

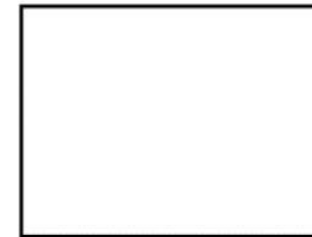
- Relación largo / ancho del elemento
- Muy alargado → pierde precisión



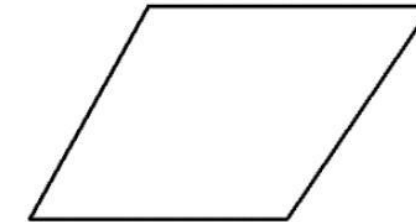
Equilateral Triangle



Highly Skewed Triangle



Equiangular Quad



Highly Skewed Quad



Condiciones de frontera e iniciales



Definen el problema que realmente resolvemos

Condiciones de frontera

Definen lo que pasa en los **bordes del sistema**

- Temperatura fija
- Flujo de calor
- Entrada / salida de aire
- Fuerzas o restricciones

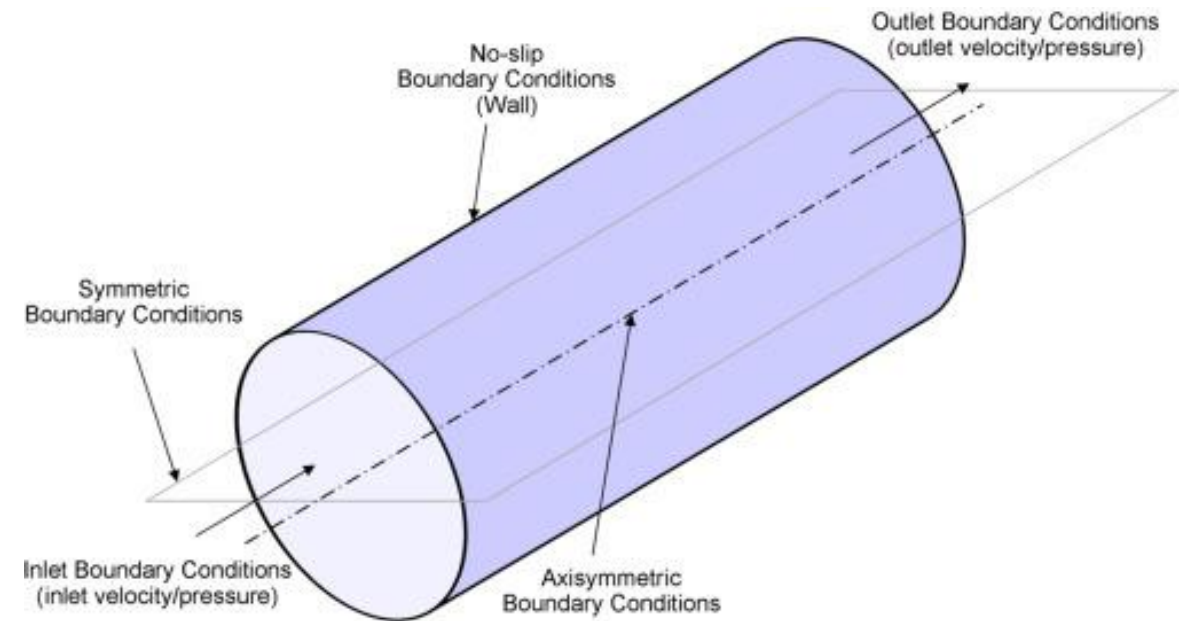
Estacionarios

Condiciones iniciales

Definen el **estado inicial en el tiempo**

- Temperatura inicial
- Humedad inicial
- Velocidad inicial

Transientes
Estacionarios





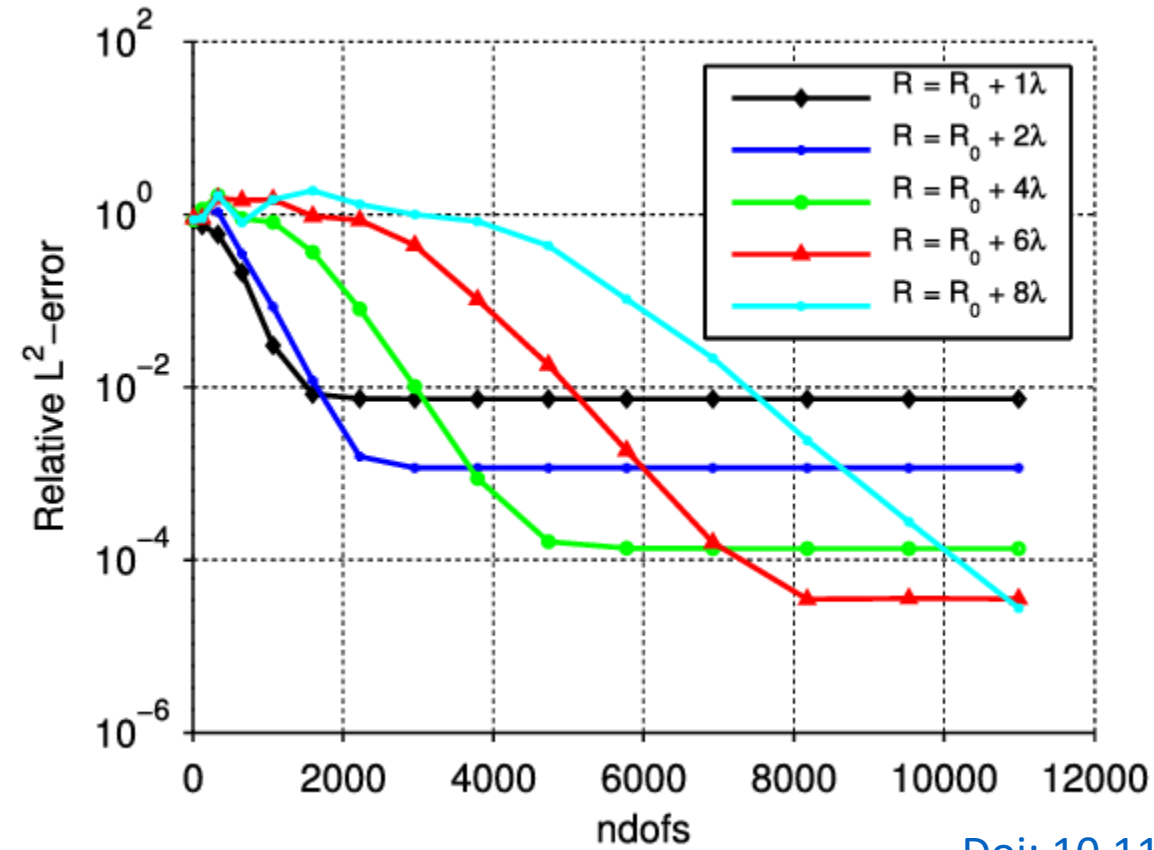
Convergencia: ¿podemos confiar en el resultado?

Un resultado es válido... solo si no depende de la malla

- Refinamos la malla
- Recalculamos
- Comparamos

Qué buscamos

Que el resultado **no cambie**
Que el error **disminuya**



[Doi: 10.1166/jctn.2011.1851](https://doi.org/10.1166/jctn.2011.1851)



Software: donde ocurre FEM

Geometría

- CAD / importación
- Simplificación del modelo

Malla

- Generación y control de calidad
- Refinamiento (h / p)

Física

- Materiales
- Condiciones de frontera e iniciales

Solución y postproceso

- Solver (lineal / no lineal / transiente)
- Resultados: campos, esfuerzos, flujos





¿Dónde se usa FEM?

Mecánica de sólidos

- Esfuerzos
- Deformaciones
- Vibraciones

Transferencia de calor

- Conducción
- Convección
- Transiente

Fluidos (CFD)

- Flujo de aire
- Turbulencia
- Distribución de velocidades

Transferencia de masa

- Difusión
- Secado
- Humedad

Electromagnetismo

- Campos eléctricos
- Ondas
- Óptica

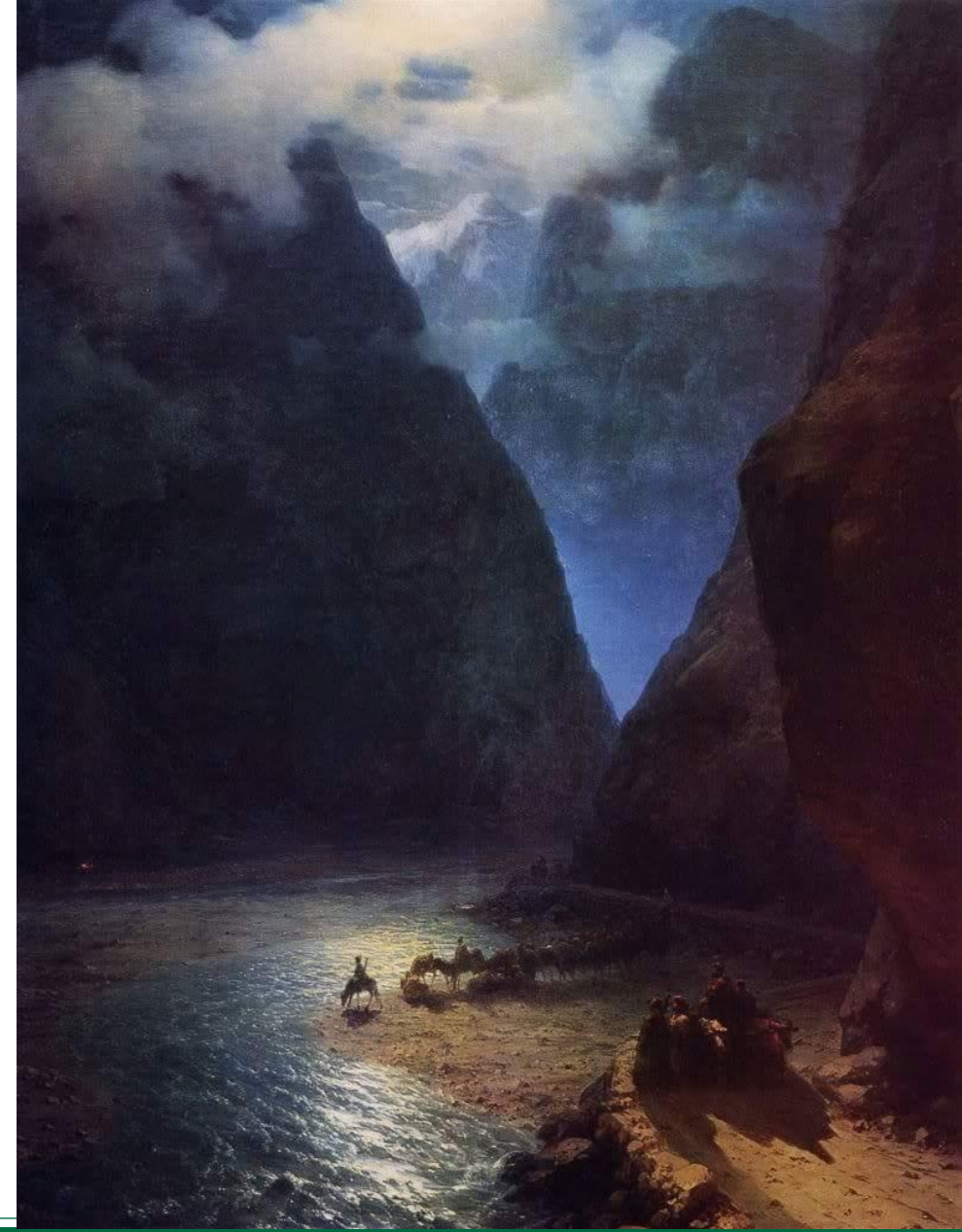
Analysis Systems
Coupled Field Harmonic
Coupled Field Modal
Coupled Field Static
Coupled Field Transient
Eigenvalue Buckling
Eigenvalue Buckling (Samcef)
Electric
Explicit Dynamics
Fluid Flow (CFX)
Fluid Flow (Fluent with Fluent Meshing)
Fluid Flow (Fluent)
Fluid Flow (Polyflow)
Harmonic Acoustics
Harmonic Response
Hydrodynamic Diffraction
Hydrodynamic Response
Magnetostatic
Modal
Modal (ABAQUS)
Modal (Samcef)
Modal Acoustics
Modal Acoustics
Random Vibration
Response Spectrum
Rigid Dynamics
Static Acoustics
Static Structural
Static Structural (ABAQUS)
Static Structural (Samcef)
Steady-State Thermal
Steady-State Thermal (ABAQUS)
Steady-State Thermal (Samcef)
Structural Optimization
Substructure Generation
Thermal-Electric
Transient Structural
Transient Structural (ABAQUS)
Transient Structural (Samcef)
Transient Thermal
Transient Thermal (ABAQUS)
Transient Thermal (Samcef)
Turbomachinery Fluid Flow
Component Systems
Autodyn
BladeGen
CFX
Discovery
Engineering Data
External Data
External Model
Fluent
Fluent (with Fluent Meshing)
Geometrv
ICEM CFD
Mechanical APDL
Mechanical Model
Mesh
Performance Map
Polyflow
Results
System Coupling
Turbo Setup
TurboGrid
Vista AFD
Vista CFD

	B	C	D	E
	Name	Physics	Solver Type	AnalysisType
1	Analysis Systems			
2	Coupled Field Harmonic	Multiphysics	Mechanical APDL	Harmonic
3	Coupled Field Modal	Multiphysics	Mechanical APDL	Modal
4	Coupled Field Static	Multiphysics	Mechanical APDL	Static
5	Coupled Field Transient	Multiphysics	Mechanical APDL	Transient
6	Eigenvalue Buckling	Structural	Mechanical APDL	Eigenvalue Buckling
7	Eigenvalue Buckling (Samcef)	Structural	Samcef	Buckling
8	Electric	Electric	Mechanical APDL	Steady-State Electric Conduction
9	Explicit Dynamics	Structural	AUTODYN	Explicit Dynamics
10	Fluid Flow (CFX)	Fluids	CFX	
11	Fluid Flow (Fluent with Fluent Meshing)	Fluids	FLUENT	Any
12	Fluid Flow (Fluent)	Fluids	FLUENT	Any
13	Fluid Flow (Polyflow)	Fluids	Polyflow	Any
14	Harmonic Acoustics	Multiphysics	Mechanical APDL	Harmonic
15	Harmonic Response	Structural	Mechanical APDL	Harmonic Response
16	Hydrodynamic Diffraction	Modal	Aqwa	Hydrodynamic Diffraction
17	Hydrodynamic Response	Transient	Aqwa	Hydrodynamic Response
18	Magnetostatic	Electromagnetic	Mechanical APDL	Magnetostatic
19	Modal	Structural	Mechanical APDL	Modal
20	Modal (ABAQUS)	Structural	ABAQUS	Modal
21	Modal (Samcef)	Structural	Samcef	Modal
22	Modal Acoustics	Multiphysics	Mechanical APDL	Modal
23	Random Vibration	Structural	Mechanical APDL	Random Vibration
24	Response Spectrum	Structural	Mechanical APDL	Response Spectrum
25	Rigid Dynamics	Structural	Rigid Body Dynamics	Transient
26	Static Acoustics	Multiphysics	Mechanical APDL	Static
27	Static Structural	Structural	Mechanical APDL	Static Structural
28	Static Structural (ABAQUS)	Structural	ABAQUS	Static Structural
29	Static Structural (Samcef)	Structural	Samcef	Static Structural
30	Steady-State Thermal	Thermal	Mechanical APDL	Steady-State
31	Steady-State Thermal (ABAQUS)	Thermal	ABAQUS	Steady-State
32	Steady-State Thermal (Samcef)	Thermal	Samcef	Steady-State
33	Structural Optimization	Structural	Mechanical APDL	Structural Optimization
34	Substructure Generation	Structural	Mechanical APDL	Substructure Generation
35	Thermal-Electric	Thermal-Electric	Mechanical APDL	Steady-State Thermal-Electric Conduction
36	Throughflow	Fluids		
37	Throughflow (BladeGen)	Fluids		
38	Transient Structural	Structural	Mechanical APDL	Transient
39	Transient Structural (ABAQUS)	Structural	ABAQUS	Transient
40	Transient Structural (Samcef)	Structural	Samcef	Transient
41	Transient Thermal	Thermal	Mechanical APDL	Transient
42	Transient Thermal (ABAQUS)	Thermal	ABAQUS	Transient
43	Transient Thermal (Samcef)	Thermal	Samcef	Transient
44	Turbomachinery Fluid Flow	Fluids	CFX	
45	Component Systems			
46	Autodyn	Explicit Dynamics	Any	Any
47	BladeGen			
48	CFX	Fluids	CFX	
49	Discovery	Any	Any	Any
50	Engineering Data	Any	Any	Any
51	External Data	Any	Any	Any
52	External Model	Any	Any	Any
53	Fluent	Fluids	FLUENT	Any
54	Fluent (with Fluent Meshing)	Fluids	FLUENT	Any
55	Geometrv	Any	Any	Any



Pausa/examen

Darial Gorge, 1862
Ivan Konstantinovich Aivazovsky

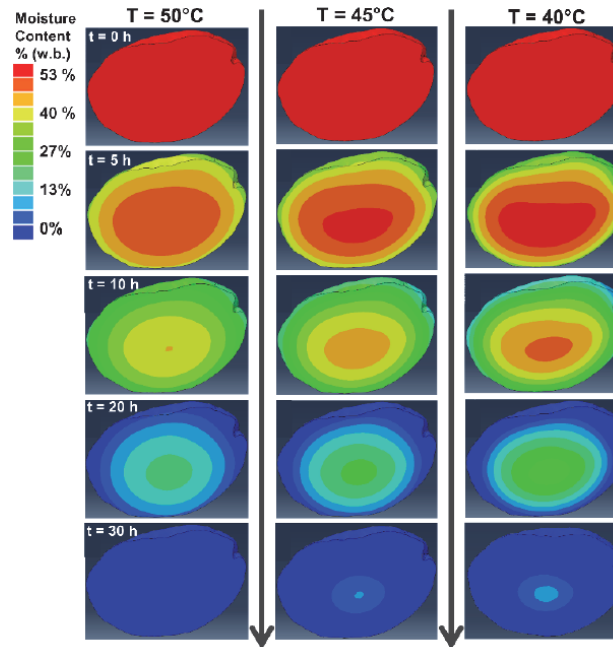
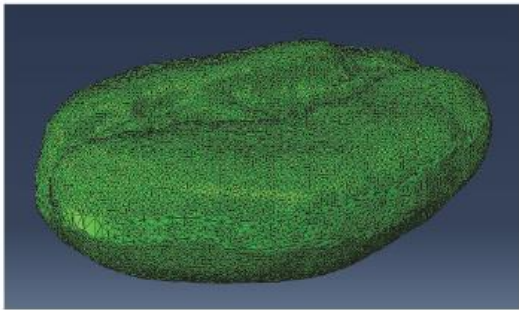
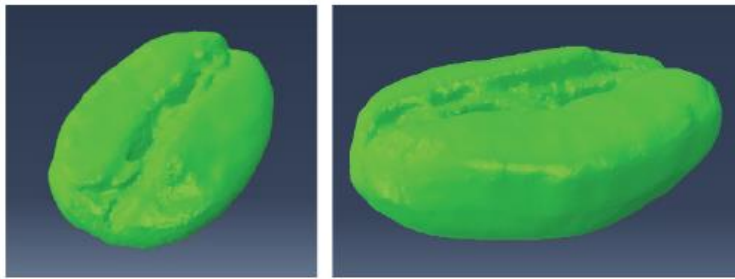




Aplicaciones en café

Secado de café (nivel de grano)

- Secado = fenómeno interno no visible
- Transferencia de calor y masa
- Geometría real del grano (3D) Modelo FEM transiente
- Gradientes internos de humedad
- Predicción del comportamiento de secado



HIGHLIGHTS

- The forced and natural convection drying processes of a single coffee grain can be predicted.
- The moisture distribution profiles depict the drying phenomena and water concentration zones.
- With accurate predictive drying curves, coffee growers can ensure high-quality coffee beans.

ABSTRACT. Different coffee drying technologies face complex tasks in ensuring an acceptable final seed moisture content. This research performed a Finite Element Analysis (FEA) study, simulating a single coffee bean's drying process as a transient mass diffusion model under mechanical and natural convection conditions, so the drying behavior and data of both case scenarios can be foreseen and controlled by a predictive Finite Element Model (FEM). A wet bean was 3D-scanned and digitized as the FEA simulation geometry; the water diffusion between the grain and the atmosphere was defined by a diffusion coefficient subject to the drying air temperature and the grain's moisture content. Three cases were studied: mechanical grain drying at three different temperatures (50, 45, and 40°C) in a forced convection environment; variable natural convection drying under environmental conditions (wet and dry season); and constant natural convection (wet and dry season), including the variation in day/night temperature and relative humidity. The results agree well with the data found in the literature, obtaining the graphical moisture distribution of the phenomena, predictive drying curves, diffusion coefficients, and isotherms. Both simulated drying scenarios provide essential information for coffee growers to improve and control their drying processes, thus obtaining high-quality grains, reducing contamination by microorganisms, and ensuring the integrity of their products.

Keywords. *Coffea arabica*, Coffee Drying, Coffee Seed, Finite Element Model, Moisture Diffusion.

When processing coffee using the wet method, drying is one of the most critical steps in the post-harvesting stages. Once the berry has been pulped, demucilaginated, and washed, it usually has a moisture content of between 60% and 50% (wb) (Parra-Coronado et al., 2008; Sfredo et al., 2005) and must be dried until it reaches 10% to 12% (wb) (Manrique et al., 2020; Rodriguez-Robles and Monroig-Saltar, 2014). After washing, due to its high water content, the coffee grain is host to an elevated biological activity. Hence, the drying process should be performed as quickly as possible to reduce the probability of spoilage and inhibit the development of microorganisms, bacteria, and mycotoxins within the grain (Batista et al., 2009). Additionally, performing the drying process quickly will help preserve its characteristics so that high-quality dry parchment coffee is obtained at the end of the process (Elhalis et al., 2021), which meets the proper commercialization and storage requirements.

To achieve proper grain dryness, coffee growers usually select between mechanical or sun drying methods to process their product (Sandeep et al., 2021). The decision is based on the amount of coffee to be dried, the climate conditions, and their economic situation. Sun drying methods are quite helpful for a reduced amount of grain to be dried since it is a rather time-intensive process (Deeto et al., 2018). Therefore, several technologies have been developed to accelerate it, including open sun dryers, parabolic, and tunnel sun-drying technologies (Oliveros-Tascón et al., 2017), as well as hybrid systems (Deeto et al., 2018; Manrique et al., 2020; Udomkun et al., 2020). Sun drying also provides a cheap and environmentally friendly solution, making it an attractive option for smallholders, such as in the case of the 563,000 Colombian coffee farming families, where 95% of them have a plot smaller than 5ha (Bravo-Monroy, 2019). Despite their advantages, sun drying technologies, which are frequently regarded as stochastic processes, face numerous complications due to their direct reliance on climate conditions, which can rapidly change over time, limiting drying behavior prediction and control (Liu and Bakker-Arkema, 2001). For example, in Colombia, the harvest peak periods overlap with the wet seasons (García et al., 2014), which are

Submitted for review on 25 April 2022 as manuscript number PRS 15156; approved for publication as a Research Article by Associate Editor Dr. Griffiths Anungdu and Community Editor Dr. Sudhagar Mani of the Processing Systems Community of ASABE on 10 July 2022.

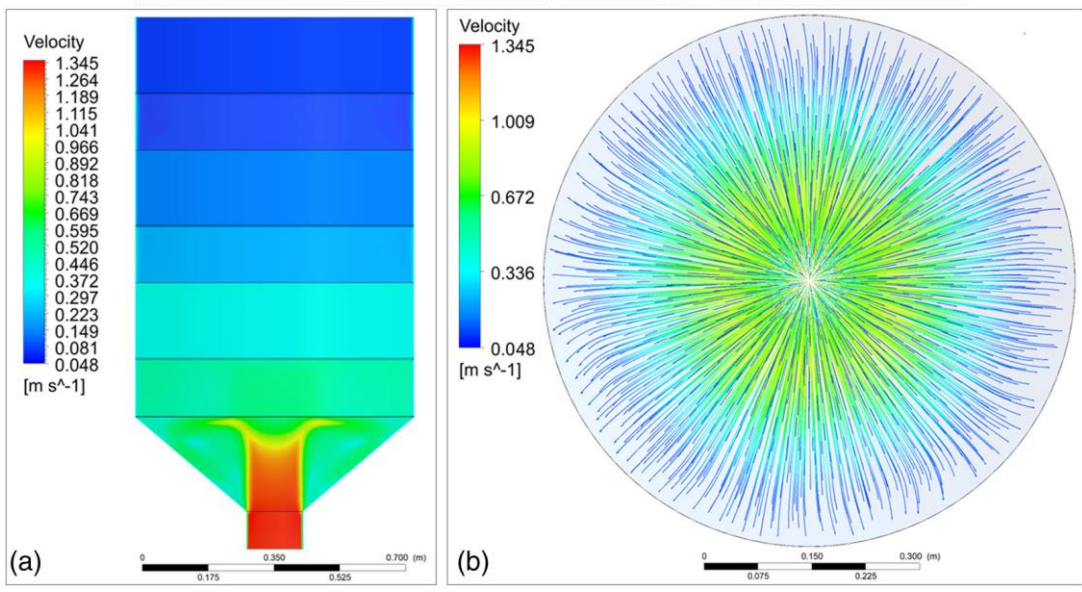
<https://doi.org/10.13031/ja.15156>.



Aplicaciones en café

Diseño y análisis de secadores

- Secado no uniforme en equipos tradicionales
- Flujo de aire como variable crítica
- Modelado FEM + CFD del secador
- Distribución de velocidad y presión
- Identificación de zonas muertas
- Evaluación de configuraciones geométricas
- Optimización del diseño del secador



Received: 29 March 2022 | Revised: 21 June 2022 | Accepted: 23 August 2022
 DOI: 10.1111/fpe.14161

ORIGINAL ARTICLE

Journal of Food Process Engineering | WILEY

Improving the drying performance of parchment coffee due to the newly redesigned drying chamber

Eduardo Duque-Dussán ^{ORCID} | Jan Banout ^{ORCID}

Department of Sustainable Technologies, Faculty of Tropical AgriSciences, Czech University of Life Sciences Prague, Prague - Suchbát, Czech Republic

Correspondence
 Jan Banout, Department of Sustainable Technologies, Faculty of Tropical AgriSciences, Czech University of Life Sciences Prague, Kamycka 129, Prague - Suchbát 16500, Czech Republic.
 Email: banout@ftz.czu.cz

Funding information
 Internal Grant Agency of the Faculty of Tropical AgriSciences; Czech University of Life Sciences Prague, Grant/Award Number: 20223109

Abstract

The Colombian coffee growers face many complications when using traditional open-sun drying techniques such as post-harvest process delays or incomplete grain dryness because of climate conditions. Therefore, local workshops began fabricating low-capacity dryers simulating the industrial equipment working principles. One of the most commercialized units is a triple tray rectangular-shaped dryer with a 31.25 kg capacity of dry parchment coffee per batch, providing the issue with an acceptable solution. However, it was redesigned into a circular shape holding a lower grain bed thickness and a vertical air inlet with a diffusive tray. Both units were simulated using the Thompson and the Michigan State University grain drying mathematical models to obtain their theoretical drying time. Then, a computational fluid dynamics simulation was conducted, attaining the unit's drying air behavior, the circular dryer exhibited notable drying times reduction and even air distribution, optimizing the dryer's performance, representing a benefit for the coffee-growing farmers.

Practical Applications

A cylindrical arranged coffee dryer with a vertical air inlet reduces the drying time of the grain, allowing a better rentability of the grower and improves the air distribution inside the equipment, meaning that the moisture removal will occur uniformly, safeguarding that the product's final moisture content meets the required conditions for safe storage.

KEYWORDS

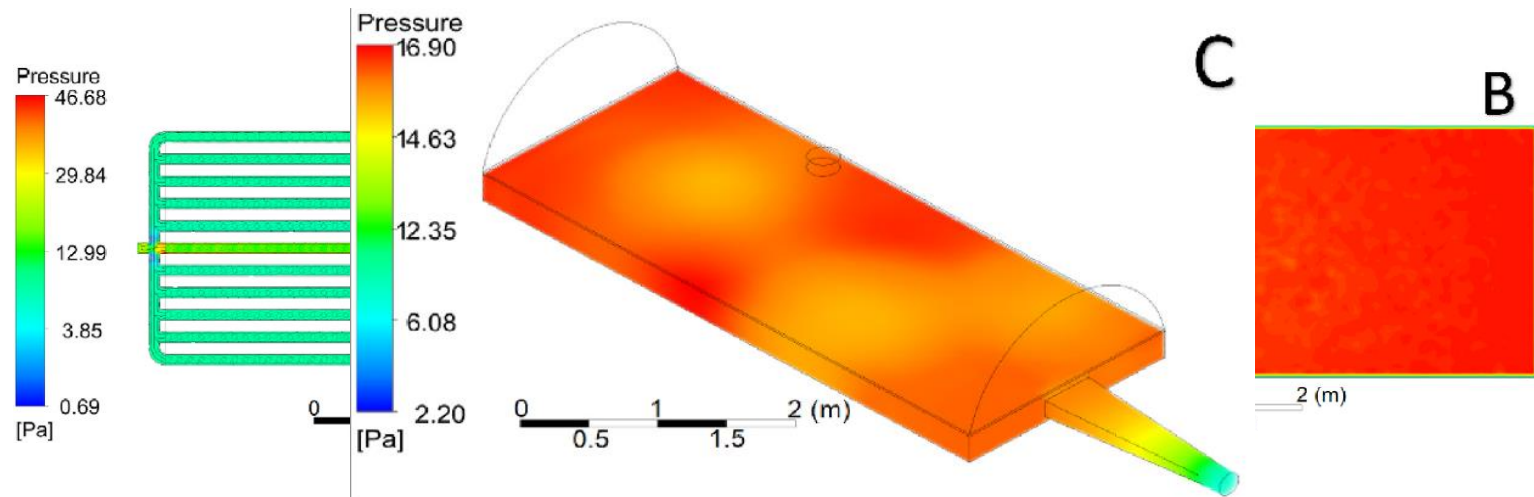
CFD simulation, *Coffea arabica*, deep bed dryer, mechanical dryer, moisture removal



Aplicaciones en café

Secador híbrido (solar + biomasa)

- Limitaciones del secado solar y mecánico
- Integración de energía solar y biomasa
- Modelado FEM + CFD del sistema
- Análisis del flujo en cámara plenum
- Distribución de presión y velocidad
- Identificación de altura óptima del plenum
- Mejora en uniformidad del secado
- Reducción significativa del tiempo de secado



Design and evaluation of a hybrid solar dryer for postharvesting processing of parchment coffee

Eduardo Duque-Dussán^a, Juan R. Sanz-Uribe^b, Jan Banout^{a,*}

^a Department of Sustainable Technologies, Faculty of Tropical Agrisciences, Czech University of Life Sciences Prague, Kamýčská 129, Prague, Suchbát, 16500, Czech Republic
^b National Coffee Research Center - CENICAFE, Km. 4 vía Chirichinó-Manizales, Manizales, Caldas, Colombia

ARTICLE INFO

Keywords:
 Biomass
 Coffee
 Coffee drying
 Hybrid dryer
 Tunnel dryer
 Mechanical drying

ABSTRACT

Due to the extended drying time open-run and solar drying of coffee procedures undergo, the development of microorganisms, mycotoxins and molds threaten the product. Alternatives such as mechanical dryers are available, nevertheless, their running costs and setups are usually expensive and unaffordable for small-scale coffee growers. Therefore, this research aimed to design, build and evaluate a hybrid solar dryer which mixes solar and mechanical drying principles. It uses a traditional solar tunnel-type dryer as a base featuring a biomass burner which uses coffee trunks left from the yearly crop renovation as biofuel. A heat exchanger heats the drying air, afterwards blown into a plenum chamber that homogenizes the air's static pressure before crossing the coffee bed, ensuring an even moisture removal. Also, the hybrid unit includes a photovoltaic system to obtain a fully self-sufficient drying unit. The newly developed dryer was tested under three different configurations: Solar and mechanical day and night (C1), solar during the day and mechanical during the night (C2) and fully solar with non-mechanical aid (C3). The results displayed a notable drying time reduction in the three evaluated configurations: C1 reduced the drying time by 70.47%, C2 by 45.75% and C3 by 21.5%. Also, the predictive model for different plenum chamber heights was obtained through computational fluid dynamics simulations, where the ideal height was 0.25 m. A biomass consumption of 1.9 kg h⁻¹ was registered. Also improved temperature and relative humidity profiles were achieved. Its design easily adapts to the existing tunnel and parabolic-type solar dryers.

1. Introduction

It is widely recognized that wet coffee processing preserves the grain's natural flavours and organoleptic properties while providing a better-quality coffee [1]. Farmer to farmer, the process differs; still, the stages are generally as follows: ripe berry detachment (selective harvest), pulping the berry to remove the fruit flesh (Mesocarp) and outer skin (Exocarp), removing the seed-covering mucilage by natural or enzyme accelerated degradation (fermentation) or mechanical principles, washing and drying [2]. As the wet parchment coffee usually holds an average moisture content of 53–55% (wb) after washing [3], drying is usually the most challenging step since it must be lowered to 10–12% (wb) in order to meet storage and commercialization requirements while avoiding growth of microorganisms, fungi or mycotoxins, preserving the grain's quality and safety [4,5].

The most common ways to dry coffee are sun-drying and mechanical

drying [6–8]. Sun energy can be used in two main ways. To begin with, there is open sun-drying, when the coffee producer spreads the beans out on an open surface and lets the sun and natural air convection remove the excess moisture. This configuration is also seen in fruit, meat, and vegetable drying [9].

However, this setup is not recommended due to the many factors that could threaten the product: animals, pests, rain, and a low level of process control. Thus, solar dryers emerged as the second form of solar energy use. Solar-drying methods include direct, indirect, mixed [10], and hybrid drying [11,12]; parabolic and tunnel dryers are the most common [13,14]. By using these dryers, the product can be dried more efficiently while mitigating the threats mentioned above. Nonetheless, these dryers are still weather-dependent and can pose an issue. For example, in many Latin-American countries, the peak coffee harvest coincides with the rainy season [15], making coffee drying more difficult.

* Corresponding author.

E-mail addresses: duque_dusman@ftz.czu.cz (E. Duque-Dussán), JuanR.Sanz@cafecolombia.com (J.R. Sanz-Uribe), banout@ftz.czu.cz (J. Banout).

<https://doi.org/10.1016/j.renene.2023.110961>

Received 15 March 2023; Received in revised form 22 June 2023; Accepted 26 June 2023

Available online 27 June 2023

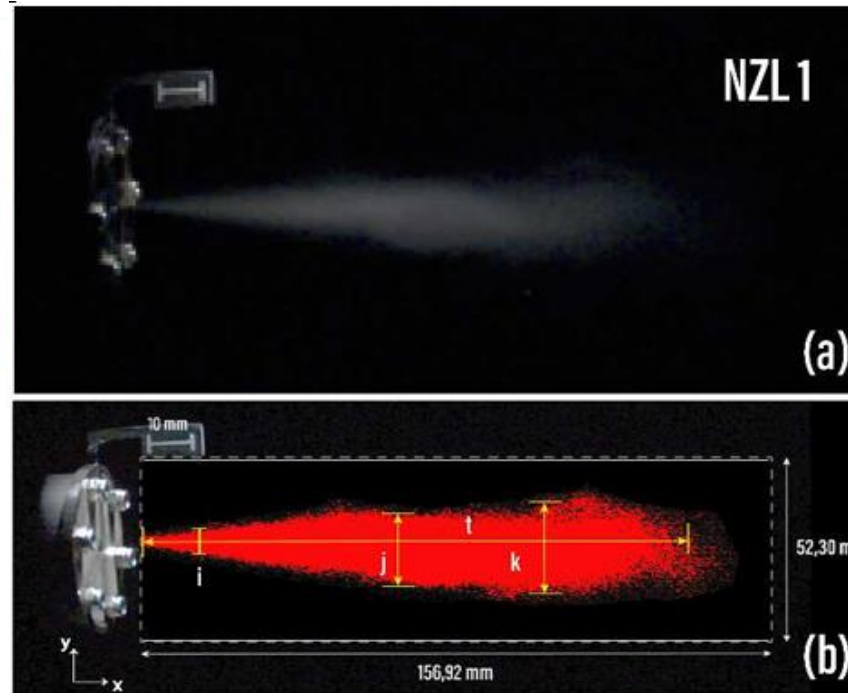
0960-1481/© 2023 Elsevier Ltd. All rights reserved.



Aplicaciones en café

Boquilla neumática para cosecha

- Limitaciones de la cosecha mecánica
- Interacción no invasiva
- Diseño paramétrico
- CFD del chorro de aire
- Presión, velocidad y frecuencia
- Vibraciones controladas
- Optimización geométrica
- Desprendimiento selectivo



Article

Optimizing Harvesting Efficiency: Development and Assessment of a Pneumatic Air Jet Excitation Nozzle for Delicate Biostructures in Food Processing

Carlos I. Cardona ¹, Héctor A. Tinoco ^{1,2,3}, Luis Perdomo-Hurtado ¹, Eduardo Duque-Dussán ⁴ and Jan Banout ^{4,*}

¹ Experimental and Computational Mechanics Laboratory, Universidad Autónoma de Manizales, Edificio Fundadores, Manizales 170001, Colombia; carlosi.cardona@autonoma.edu.co (C.I.C.); htinoco@autonoma.edu.co (H.A.T.); lperdomo@autonoma.edu.co (L.P.H.)
² Institute of Physics of Materials, Sciences Academy of the Czech Republic, 61600 Brno, Czech Republic
³ Central European Institute of Technology, 61600 Brno, Czech Republic
⁴ Department of Sustainable Technologies, Faculty of Tropical AgriSciences, Czech University of Life Sciences Prague, Kamýcká 129, 16500 Prague, Czech Republic; duque_dussan@tz.czu.cz
* Correspondence: banout@tz.czu.cz

Abstract: This study presents a new pneumatic air jet excitation nozzle, specifically designed for food processing applications. The device, which uses compressed air equipment and a precision solenoid valve, controls air discharge through a parametric air jet nozzle. Tests showed that the device could achieve shooting frequencies in the 40–45 Hz range, with operational pressures between 5 and 7 bar. A sensor system was used to measure the force generated by the device at different frequencies and pressures. Using the Design of Experiments (DOE) methodology, we identified optimal cavity designs for 5 and 6 bar pressures. These designs outperformed others in generating uniform force and maintaining consistent vibration voltage behavior. This highlights the efficacy of our approach in enhancing device performance under different conditions. The device's practical application in food processing was demonstrated, particularly in delicate tasks such as the selective harvesting of sensitive crops like coffee fruits. The precise vibrations generated by the device could potentially enhance harvesting efficiency while significantly reducing mechanical damage to plants. The results position the device as a compelling proof of concept, offering an alternative method for exciting biostructures in food processing. This device opens up new possibilities in agricultural and biological fields, providing a non-intrusive and practical approach to manipulating and interacting with delicate, contactless structures, with a specific focus on improving food processing efficiency and quality.

Keywords: precision nozzle design; pneumatic air jet excitation; shooting frequencies; contactless vibrations generation; food processing; harvesting efficiency



Citation: Cardona, C.I.; Tinoco, H.A.; Perdomo-Hurtado, L.; Duque-Dussán, E.; Banout, J. Optimizing Harvesting Efficiency: Development and Assessment of a Pneumatic Air Jet Excitation Nozzle for Delicate Biostructures in Food Processing. *Foods* **2024**, *13*, 1458. <https://doi.org/10.3390/foods13101458>

Received: 15 April 2024
Revised: 29 April 2024
Accepted: 1 May 2024
Published: 8 May 2024



Copyright: © 2024 by the authors. Licensee MDPI, Basel, Switzerland. This article is an open access article distributed under the terms and conditions of the Creative Commons Attribution (CC BY) license (<https://creativecommons.org/licenses/by/4.0/>).

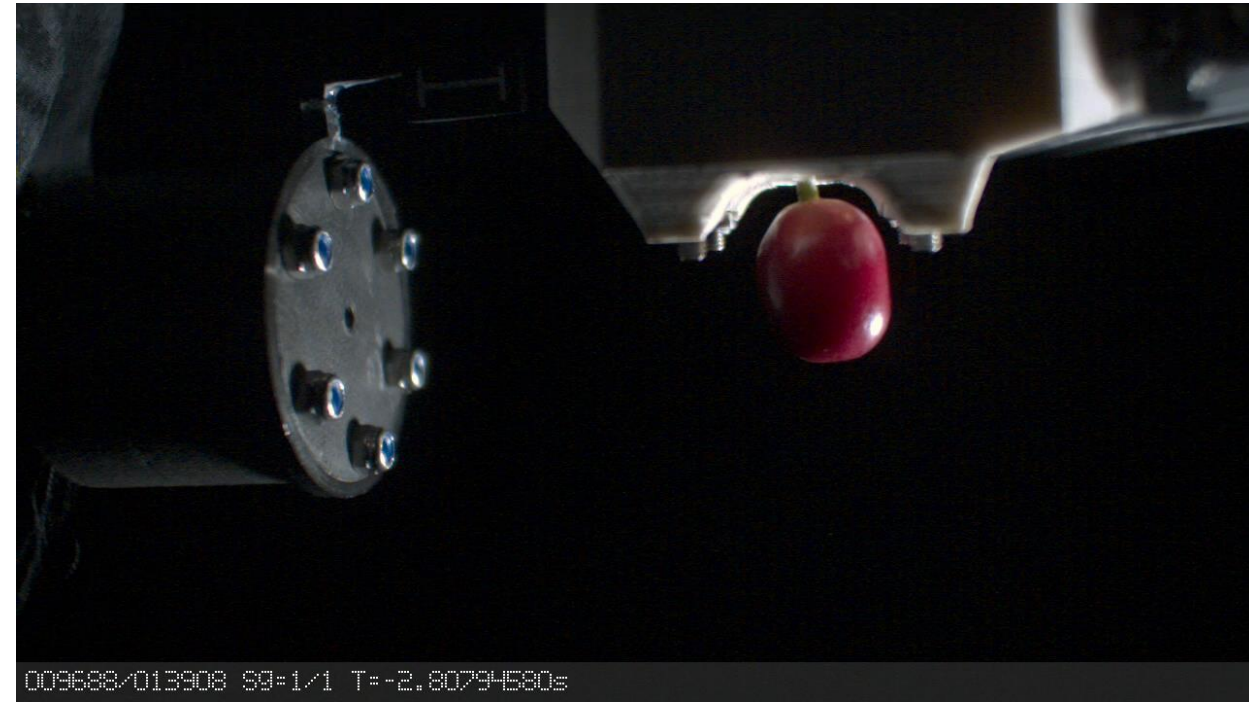
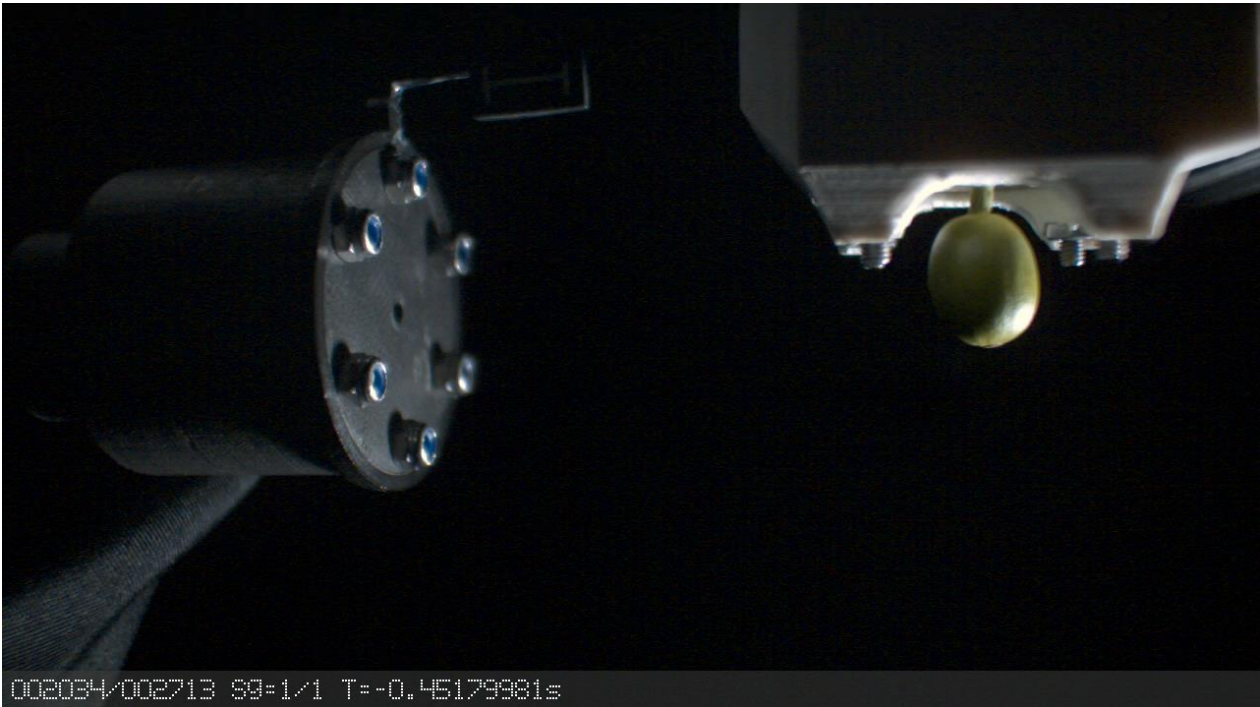
1. Introduction

Several methods of contactless mechanical excitation have been studied, where ultrasound wave propagation [1], air [2], magnetic [3], and laser pulses [4] acted as energy sources. These have been proposed to generate vibrations over diverse kinds of structures. All these techniques are widely used to diagnose structural integrity, detect failure, characterize dynamic properties, and predict behavior [5–8]. For instance, a laser ablation excitation mechanism was developed [5] to characterize a rotating disk on a hard drive. This type of excitation uses a high-power YAG pulse laser that generates an impulse force on the disk surface, and vibrations were measured using a Doppler effect laser vibrometer. In a similar approach to designing a resonator, a laser diode excites the specimen, generating lateral vibrations and leading to four resonance frequencies between 0.1 and



Aplicaciones en café

Boquilla neumática para cosecha





Aplicaciones en café

Propiedades elásticas del café

ORIGINAL ARTICLE

Determination of Elastic Properties of *Coffea arabica* L. var. Castillo Bean-Mesocarp Using Finite Element Analysis and Experimental Methods

Eduardo Duque-Dussán^{1,2} | Alexander Rincón-Jimenez³ | Hector Andrés Tinoco³ | Carlos Iván Cardona³ | Carlos A. Ibarra³ | José Luis Rodríguez-Sotelo⁴

¹Postharvest Discipline, National Coffee Research Center – Cenicafé, Mantzales, Colombia | ²Department of Sustainable Technologies, Faculty of Tropical Agrisciences, Czech University of Life Sciences Prague, Suchbát, Czech Republic | ³Experimental and Computational Mechanics Laboratory, Universidad Autónoma de Mantzales, Antigua Estación del Ferrocarril, Mantzales, Colombia | ⁴Grupo de Automática, Universidad Autónoma de Mantzales, Antigua Estación del Ferrocarril, Mantzales, Colombia

Correspondence: Eduardo Duque-Dussán (eduardo.duque@cafede colombia.com; duque_dussan@tz.czu.cz)

Received: 7 October 2025 | Revised: 24 November 2025 | Accepted: 10 December 2025

Keywords: coffee fruit | compression tests | finite element analysis | mechanical properties | ripening stages

ABSTRACT

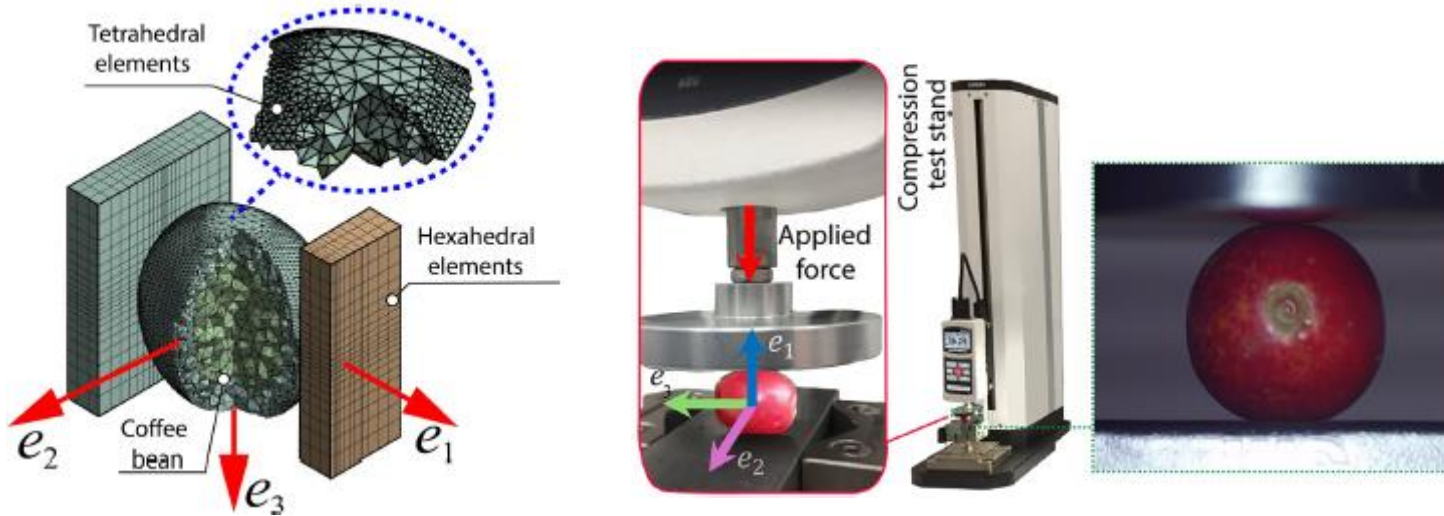
This research studies *Coffea arabica* L. var. Castillo coffee fruit elastic properties using experimental techniques and finite element analysis (FEA). Young's modulus and Poisson's ratio for both fruit and bean at several stages of ripeness were measured through indentation and compression testing to evaluate mechanical behavior. Three simulation approaches in FEA were utilized, successively developing material characterizations from isotropic to orthotropic. The first simulation, with isotropic material characterizations, showed a significant deviation in agreement with experimental observations. In contrast, the second simulation, with incorporated properties derived through indentation, showed increased accuracy but continued to have discrepancies for overripe and ripe fruits. By contrast, in the third simulation, an orthotropic model with parametric variation in Young's modulus closely agreed with experimental observations in terms of compression, accurately depicting anisotropy in mechanical properties in coffee fruit. The observations can be utilized in optimizing mechanical harvesting and postharvest processing machinery, such as pulpers and sorters, with consideration for mechanical features in relation to stage of ripeness. Future studies with increased refinement in representing materials and including dynamic loading will have a significant impact in terms of predictive accuracy relevant to coffee processing operations.

1 | Introduction

Coffee is one of the most consumed beverages and a key global commodity, playing a crucial role in economic development and livelihoods, particularly in producing countries (Amrouk et al. 2025; Borrella et al. 2015; International Coffee Organization 2023). Colombia, recognized for its high-quality *Coffea arabica* L. production, holds a prestigious position in the

global coffee industry due to its consistently high sensory standards (Suárez et al. 2022). However, Colombian coffee farmers face significant challenges, including the spread of diseases such as coffee leaf rust (*Hemileia vastatrix*) and coffee berry disease (CBD), both of which threaten productivity and sustainability (Atallah et al. 2018; Avelino et al. 2015; Ferrucho et al. 2024; Góngora et al. 2023; Talhinhos et al. 2017). While CBD has not yet been detected in Colombia (Quiroga-Cardona et al. 2024), the

- Comportamiento mecánico del fruto y grano
- Ensayos de compresión e indentación
- Modelado FEM del fruto
- Comparación modelo–experimento
- Evaluación isotrópica vs ortotrópica
- Identificación de propiedades elásticas
- Influencia del estado de maduración
- Base para diseño de maquinaria



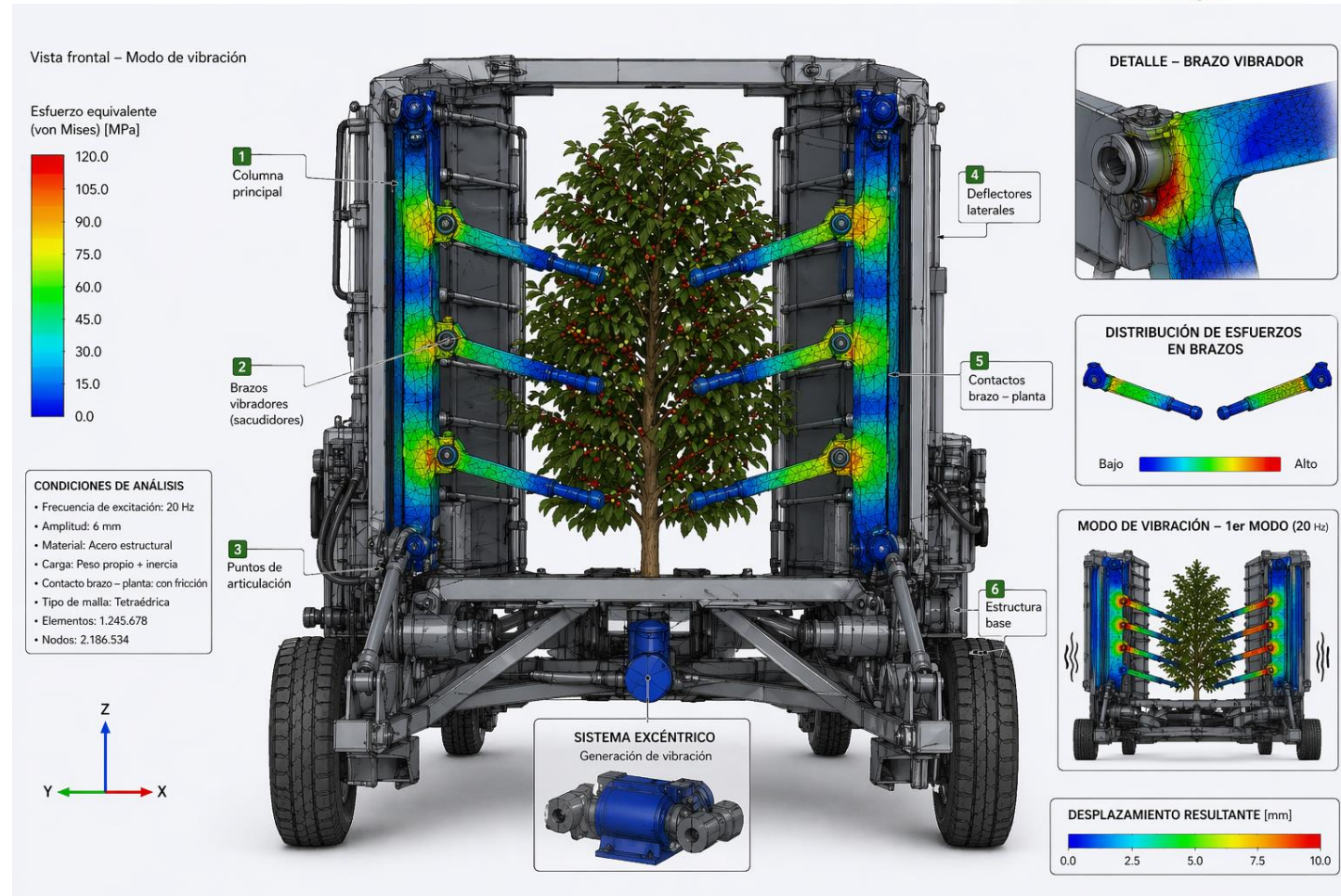


Aplicaciones en curso

Hacia la mecanización del café



- Integración FEM en procesos poscosecha
- Modelado de interacción máquina-planta
- Análisis de vibraciones para desprendimiento
- Estudio de esfuerzos en estructuras agrícolas
- Diseño conceptual de sistemas de cosecha
- Optimización de componentes mecánicos
- Reducción de daño en fruto y planta
- Base para mecanización en caficultura





Cenicafé[®]
Centro Nacional de Investigaciones de Café



cenicafe.org



Cenicafé FNC



@cenicafe



cenicafé



CenicaféFNC



@cenicafefnc